

The Temperature Dependence of the Work Functions  
of the Monovalent Noble Metals

by

Clarence Robert Crowell

A thesis submitted to the Faculty of Graduate  
Studies and Research at McGill University  
in partial fulfilment of the requirements  
of the degree of  
Doctor of Philosophy

Eaton Electronics Research Laboratory

McGill University

April 1955

## INDEX

	Page
ABSTRACT	i
INTRODUCTION	1
THEORY OF THE TEMPERATURE DEPENDENCE OF THE WORK FUNCTION	4
The Surface Dipole Layer	6
The Thermal Expansion Effect	8
The Effect of Thermal Excitation on the Fermi Energy	12
The Effect of Atomic Vibrations on the Chemical Potential	15
The Electrostatic Effect of Thermal Vibrations at Constant Volume	20
Theoretical Results	23
EXPERIMENTAL MEASUREMENTS ON THE MONOVALENT NOBLE METALS	
Introduction	27
Experimental Method	28
Vacuum Procedure	41
Measurements	44
CONCLUSIONS	54
APPENDICES	
I    Sensitivity of the Dynamic Capacitive Method	56
II   The Time for Contamination of Clean Surfaces	59
III  Analysis of Results	63
REFERENCES	70
ACKNOWLEDGMENTS	72

ABSTRACT

A theory to explain the temperature dependence of the work function of the monovalent metals has been developed assuming a free-electron approximation for the valence electrons, and a Debye model for the thermal vibrations of the ion cores. The theory predicts that the electrostatic effect of thermal vibrations is the chief contribution to the temperature coefficient of the work function, all other contributions being either negligible or cancelling. Agreement between theory and experiment was obtained from observations made on silver and copper films but not from less reliable measurements made on gold films. Measurements were taken over the temperature range 300°K to 800°K using a capacitive contact potential method. Fresh surfaces were prepared in a sealed off system at maximum pressures of  $6 \times 10^{-9}$  to  $1.2 \times 10^{-7}$  millimeters of mercury. Contact potentials were measured immediately afterwards at pressures of the order of  $10^{-9}$  millimeters of mercury. The results obtained from successively evaporated silver and copper films were reproducible and free from drift, but the gold films were not satisfactory in either respect. Approximately consistent results, however, were obtained from three successively deposited gold films. The results corrected for the absolute thermoelectric power of platinum ( $-7.3 \times 10^{-6}$  volts/°K) were  $-134 \times 10^{-6}$ ,  $-57 \times 10^{-6}$  and  $9 \times 10^{-5}$  electron volts/°K for silver, copper and gold films respectively.

The Temperature Dependence of the Work Functions of the  
Monovalent Noble Metals

INTRODUCTION

The work described in this thesis falls into two sharply defined categories: theory and experiment. A theory of the temperature dependence of the work functions of monovalent metals is developed in the first part of the thesis and experimental measurements on the monovalent noble metals are described in the second part.

The temperature dependence of the work function is of interest as a property of a metal surface because it can afford a check on solid state theory and also because it is one of the factors which affects the thermionic emission of a metal surface.

The existing theories of the temperature dependence of the work function are very rudimentary. These theories have concentrated for the most part on calculating the effect of thermal expansion and the effect of the electronic specific heat. In most cases effects of lattice vibrations at constant volume have been neglected. It appears that these should be as large or larger than the effects which have been considered. These theories have been carefully reviewed and several valuable suggestions advanced by Herring and Nichols<sup>1</sup> in their review article on thermionic emission. The situation which confronted the author, was, however, one in which all the effects could not be calculated quantitatively for any one metal.

The theoretical portion of this thesis describes the development of the approach suggested by Herring and Nichols. A new expression is derived for the effect of thermal expansion. This expression includes the effect of expansion on a surface dipole layer as predicted from Smoluchowski's<sup>2</sup> theoretical calculation of the dipole layer and also

considers the correlated electron interactions as formulated in the Wigner-Bardeen<sup>3</sup> calculation of the work functions of the alkali metals. The effect of thermal vibrations at constant volume on the chemical potential is deduced theoretically for the first time. These developments allow all the contributions to the temperature dependence of the monovalent metals to be calculated and also show that a virtual cancellation of the effects of thermal expansion and of thermal vibrations on the chemical potential should be expected at all temperatures in the case of the monovalent metals. The major contribution to experimental values of the temperature coefficient of the work function must then be interpreted as the electrostatic effect of thermal ion core vibrations at constant volume. Comparison of theoretical and experimental values shows that for silver and copper this interpretation is qualitatively consistent.

In measuring the temperature dependence of the work function, the choice of method is very important. At high temperatures the cooling effect of electron emission has been used, while at low temperatures photoelectric measurements have been made. Two other methods have been used which do not require emission of electrons from the test surface. In a diode changes in the anode work function can be observed by measuring the accompanying shifts in the space charge limited characteristics. The change in contact potential between two metal surfaces has also been used to measure changes in work function.

The contact potential method is the most satisfactory way of measuring the temperature dependence of the work function. If a method is used which requires the emission of electrons from the surface being studied, the measured work function of a contaminated or polycrystalline surface can be temperature dependent even if no change occurs in the

actual work function. This can occur because a temperature dependent emissive mean work function is measured and not the arithmetic mean of the work function. Contact potential methods on the other hand measure the arithmetic mean and can only yield a temperature variation if there is a change in the actual work function of the surface. This explains the author's choice of a contact potential method in this work. The method using the shift in diode characteristics could have been used. It is difficult, however, to obtain accurate results from this method if the measurements are made in the space charge limited region far removed from the retarding potential region. This must be done if changes in the arithmetical mean of the anode work function are to be measured.

The existing published measurements of the temperature dependence of the work function are of somewhat dubious accuracy since all were made prior to 1940 and the experimenters could not take advantage of more recent developments in vacuum technique. These measurements were all subject to contamination effects due to either the fact that they were made using inadequate vacua or that the methods of preparation of the test surfaces could not ensure that they were clean. The author therefore took great care to produce adequate vacua and to deposit fresh metal surfaces by evaporation. Measurements were made under conditions where contamination effects could be detected if they were present.

The experimental results obtained from silver and copper films were reproducible and no contamination effects were apparent. The agreement between theoretical and experimental results is good for these metals. The theory cannot explain the results obtained from gold films. The measurements on gold, however, lacked the reproducibility of the results from copper and silver films and also showed definite signs of contamination.

## THEORY OF THE TEMPERATURE DEPENDENCE OF THE WORK FUNCTION

The ideas presented here are based on existing theories of the solid state. A synthesis and expansion of these theories results in an expression for the temperature coefficient of the work function of the monovalent metals.

In the following treatment the zero of electrostatic potential will be considered to be the potential in a field free region far removed from the metal under consideration. The work function of a crystal face of the metal will then be

$$\phi = W_0 - \bar{\mu} \quad (1)$$

where  $W_0$  is the potential energy of an electron in a region of zero electric field just outside the crystal face, and  $\bar{\mu}$  is the electrochemical potential of the electrons in the metal. In general  $W_0$  need not be zero because different surface dipole layers may exist on different crystal faces of the metal. The electrochemical potential of the electrons in a system at a temperature  $T$  having a volume  $V$  per unit cell and containing  $Z$  electrons per unit cell is defined by the equation

$$\bar{\mu} = \left( \frac{\partial F}{\partial Z} \right)_{T, V} \quad (2)$$

$F$  is the Helmholtz free energy per unit cell of the system.  $\bar{\mu}$  can be expressed as the sum of terms due to the kinetic energy of the electrons, the average electrostatic potential energy of the electrons in the metal, and the correlated individual electrostatic interactions between the electrons. The chemical potential is

$$\mu = \bar{\mu} - W_1 \quad (3)$$

where  $W_i$  is the average potential energy of an electron inside the metal.  $\mu$  is thus composed of the terms in  $\bar{\mu}$  involving the kinetic energies and correlated electrostatic interaction energies of the electrons. If

$$W = W_0 - W_i \quad (4)$$

then

$$\phi = W - \mu \quad (5)$$

In the case of a free electron gas, if the electron interactions can be approximated by a contribution to the average electrostatic potential,  $\mu$  is the Fermi kinetic energy. A more complete consideration of  $\mu$  and  $\bar{\mu}$  can be found in Reference 1.

When considering the temperature dependence of the work function both temperature and volume effects are important. This is because the work function of a metal is always measured in a vacuum (i.e. at constant pressure) to avoid the effects of surface contamination. Thus the temperature coefficient of work function will be

$$\frac{d\phi}{dT} = \left( \frac{\partial \phi}{\partial T} \right)_V + \left( \frac{\partial \phi}{\partial V} \right)_T \frac{dV}{dT} \quad (6)$$

General thermodynamic reasoning yields only one numerical restriction to the temperature dependence of the work function. This occurs as a result of Nernst's Heat Theorem which can be stated in the following form: near absolute zero the entropy  $S$  of a crystal approaches a limiting value independent of the electron concentration.

Since

$$S = - \frac{\partial F}{\partial T} \quad (7)$$

$$\text{then } -\frac{\partial \bar{\mu}}{\partial T} = -\frac{\partial^2 \bar{\mu}}{\partial Z \partial T} = \frac{\partial S}{\partial Z} \rightarrow 0 \quad \text{as } T \rightarrow 0 \quad (8)$$

Also

$$\frac{dV}{dT} \rightarrow 0 \quad \text{as } T \rightarrow 0 \quad (9)$$

Changes in  $W_0$  arising from the surface dipole layer are also produced only by a change in entropy or volume of the metal. Since these variables reach stationary values as  $T \rightarrow 0$ ,

$$\frac{d\phi}{dT} \rightarrow 0 \quad \text{as } T \rightarrow 0 \quad (10)$$

Every postulated mechanism for producing a temperature coefficient of work function will be found to satisfy this condition.

Previous theoretical treatments consider a total of five contributions to the temperature coefficient of work function. These are:

the effect of changes in the surface dipole layer;

the effect of thermal expansion on the volume dependent contributions to the work function;

the effect of thermal excitation on the Fermi kinetic energy;

the effect of lattice vibrations on the chemical potential; and

the electrostatic effect of thermal lattice vibrations.

These contributions will be considered separately in the following sections.

#### The Surface Dipole Layer

The electron charge distribution in the surface cells of a metal cannot be expected to be the same as the interior charge distribution.

This is because the valence electrons tend to move away from a metal to reduce the total energy of the system. The resultant charge distribution is equivalent to the effect of a charge density in the surface cells like that in the interior plus the effect of a surface dipole layer. Such dipole layers are responsible for differences in the work functions of different crystal faces of a metal. The best estimates of the size of dipole layers show that they are a fraction of a volt for the alkali metals and can be considerably larger for other metals. Some of these values have been deduced by comparing experimental values of the work function with those predicted by theories based on volume considerations alone, ascribing the difference to the dipole layer (Herring and Nichols<sup>1</sup>). An approximate direct calculation by Bardeen<sup>4</sup> yielded a value of 0.15 electron volts for the 110 face of a sodium crystal. Neglecting exchange and correlation effects Smoluchowski<sup>2</sup> found that crystal faces with a dense population of atoms tended to have large dipole layers which increased the work function.

The variation of a dipole layer with temperature should be chiefly the result of thermal expansion. The effect of thermal excitation on the spreading of the charge distribution has been shown<sup>5</sup> to be negligible. If the surface charge distribution expands uniformly with the rest of the metal,

$$\frac{\partial D}{\partial V} \frac{dV}{dT} = -D\alpha \quad (11)$$

$D$  is the contribution of the surface dipole layer to the work function and  $\alpha$  is the linear expansion coefficient of the metal. This is the behaviour predicted by Smoluchowski's theory assuming isotropic expansion

of the metal. The temperature coefficient of different crystal faces should thus differ an amount

$$\frac{\partial \Delta \phi}{\partial V} \frac{dV}{dT} = -\Delta \phi \alpha \quad (12)$$

where  $\Delta \phi$  is the difference between their work functions. Since typical values of  $\Delta \phi$  are of the order of a fraction of a volt for metals thus far investigated (e.g. Cu<sup>6</sup>, Ag<sup>7</sup>, W<sup>8</sup>), differences in the temperature coefficient of work function should be difficult to detect unless the coefficient of expansion is large. The effect of contamination on a surface is like that of an additional dipole layer. If this is stable and only changes the work function slightly, the change in temperature coefficient predicted by Equation (12) will also be small. This may explain the fact that Potter's<sup>9</sup> results for tungsten were independent of the degree of contamination to the order of accuracy of his measurements.

Thus the temperature coefficient of the average work function of a slightly contaminated polycrystalline surface should be close to that of a clean single crystal face if the contamination is stable.

#### The Thermal Expansion Effect

10

As early as 1912 Richardson<sup>10</sup> suggested that thermal expansion might change the work function. Modern concepts of the solid state have resulted in four suggested theories of the thermal expansion effect. These are due to Herzfeld<sup>11</sup>, Riemann<sup>12</sup>, Wigner<sup>13</sup> and Seely<sup>14</sup>. These theories all agree as to the effect of expansion on the Fermi kinetic energy, but differences occur in the details of the variation of  $W$  and the interaction terms contributing to  $\mu$ . Wigner's treatment is the most rigorous, but

neglects the effects of the surface dipole layer, while Seely's result has a convenient form for including the effect of expansion on the surface dipole layer, but neglects some of the effects of electron interactions. An expression will now be derived which will incorporate the advantages of both theories.

According to the Wigner-Bardeen theory<sup>3</sup>, the work function of a metal is

$$\phi = \sum_i Z e^2 / r_i - V_f + D - E_f - E_{cm} - e_f \quad (13)$$

$-\sum_i Z e^2 / r_i$  is the electrostatic potential energy of a valence electron due to the attraction of the nuclei in the metal and the repulsion of the bound electrons. The nuclei and bound electrons are assumed to act as rigid ion cores having a charge  $Ze$ .

$V_f$  is the potential energy of a valence electron due to the average charge density of the other valence electrons. If the free electron approximation applies, this charge density is approximately uniform throughout the metal.

$D$ , the contribution of a surface dipole layer has already been discussed. For alkali metals it may be assumed to be small, but for the monovalent noble metals it is appreciable, judging by the discrepancy between theoretical and experimental values of  $\phi$  if it is neglected.

$E_f$  is a contribution due to the exchange energy of the valence electrons. This term partially corrects for the fact that  $V_f$  is larger than the actual repulsive effect of the other valence electrons. Because of the Pauli principle the valence electrons of like spin avoid each other, hence do not see the other electrons as a charge cloud of uniform

density. For free electrons the exchange energy is

$$E_e = -C_k e^2 / r_s \quad (14)$$

$C_k$  is a constant which depends on the momentum of the electron<sup>4</sup>.  $r_s$  is the radius of a sphere which would contain the charge of one electron if all the free electron charges in the system were uniformly distributed. Thus if  $V$  is the volume of the unit cell and  $Z$  the number of free electrons per unit cell,

$$\frac{4}{3} \pi r_s^3 Z = V \quad (15)$$

The contribution of the exchange energy to  $\mu$  is

$$E_f = -0.611 e^2 / r_s \quad (16)$$

$E_{cm}$  is a term arising from the correlation of the valence electrons. It arises from the correlated interactions of valence electrons of opposite spins. Wigner<sup>15</sup> has calculated the average correlation energy per electron for a free electron gas:

$$E_c = - \frac{0.288 e^2}{r_s + 5.1 a_h} \quad (17)$$

$a_h$  is the Bohr radius

$$a_h = \frac{h^2}{4\pi^2 m e^2} = 0.531 \text{ \AA} \quad (18)$$

The contribution of the correlation energy to  $\mu$  is

$$E_{cm} = E_c(r_s) - \frac{1}{3} E'_c(r_s) r_s \quad (19)$$

(see Seitz<sup>16</sup>, Sect. 76).

$e_f$  is the Fermi kinetic energy of the system. If a free electron approximation is assumed for the valence electrons,

$$e_f = \frac{h^2}{4m^* r_s^2} \left[ \frac{3}{2\pi} \right]^{4/3} \quad (20)$$

where  $h$  is Planck's constant and  $m^*$  is the effective electron mass (see Seitz<sup>16</sup>, Sect. 26).

Theoretical work on several of the monovalent metals (e.g. Li<sup>17</sup>, Na<sup>18</sup>, K<sup>19</sup>, and Cu<sup>20</sup>) indicates that the valence electrons are approximately free. The electrons have almost a parabolic density of states and their average charge distribution is approximately uniform throughout the metal. Thus the effect of thermal expansion should be simply a uniform expansion of the electron charge density; i.e.

$$\frac{\partial r_s}{\partial V} \frac{dV}{dT} = r_s \alpha \quad (21)$$

where  $\alpha$  is the coefficient of linear expansion. Any term depending inversely on  $r_s$  will then have a thermal expansion effect similar to that of the surface dipole layer. Differentiating Equation (13),

$$\frac{\partial \phi}{\partial V} \frac{dV}{dT} = (e_f + V_c - \phi) \alpha \quad (22)$$

where

$$V_c \alpha = - \frac{\partial E_{cm}}{\partial V} \frac{dV}{dT} - E_{cm} \alpha = - \left[ 1 - \frac{r_s(r_s + 5.1 a_h)}{(r_s + 5.1 a_h)^2} \right] E_c \alpha \quad (23)$$

Equation (22) is very similar to Seely's result

$$\frac{\partial \phi}{\partial V} \frac{dV}{dT} = (e_f - \phi) \alpha \quad (24)$$

which neglects the effects of the correlation energy.

$V_c$  and  $e_f$  are easily calculated. Since experimental values of  $\phi$  can be used, an uncertainty in the potential terms is unimportant provided these terms vary inversely with  $r_s$ .

Considerable error can be expected in the correlation energy term  $V_c$ , however, since Wigner estimated that his calculation of the average correlation energy is accurate to about 20 percent for the idealized case of free electrons.

For metals other than the monovalent metals, a quantitative calculation of the thermal expansion effect is much more difficult because the free electron approximations break down. In such cases no calculations of this effect have been made, but a qualitative observation is possible when an energy band is almost filled. Calculations of the top of energy bands as a function of lattice constant show that an electron in a state near the top should become more tightly bound to the metal as it expands, hence the thermal expansion effect should be positive.

#### The Effect of Thermal Excitation on the Fermi Energy

Thermal excitation of the electrons in a metal changes the Fermi energy of the electron distribution. The temperature coefficient

of the Fermi energy due to thermal excitation of the electrons is

$$\frac{\partial e_f}{\partial T_e} = \frac{\pi^2 k^2 T g'(e_f)}{3g(e_f)} \quad (25)$$

$g(e_f)$  is the energy density of states in the metal at the Fermi energy, and  $k$  is Boltzmann's constant. A derivation of this formula can be found in Reference 16, Section 26. As expected from more general reasoning (Equation (10)),

$$\frac{\partial e_f}{\partial T_e} \rightarrow 0 \quad \text{as } T \rightarrow 0 \quad (26)$$

When the density of states is parabolic, the electronic specific heat is

$$\gamma_V = \frac{\pi^2 k^2 T}{2 e_f} = \frac{\beta k T}{Z} \quad (27)$$

and

$$\frac{\partial e_f}{\partial T_e} = -\frac{\pi^2 k^2 T}{6 e_f} = -\frac{\beta k T}{3 Z} \quad (28)$$

$\beta k T$  is the term linear in  $T$  in the specific heat per unit cell.

Experimental values of  $\beta$  are of the order of  $10^{-4}$  for the monovalent metals, in fair agreement with the values predicted by the free electron theory<sup>21</sup>. This means that the values of this contribution to the temperature coefficient of the work function are small in comparison with  $k$  ( $= 86.17 \times 10^{-6}$  electron volts/ $^{\circ}\text{K}$ ) even at high temperatures.

Equations (27) and (28) are only valid when  $kT \ll e_f$ . For most metals this condition is satisfied even near the melting point. The

situation when  $kT$  is comparable to  $e_F$  has been investigated by Mott<sup>22</sup> and Stoner<sup>23</sup>. In a complete solution for  $\gamma_V$  and  $\partial e_F / \partial T_e$  Equations (27) and (28) contain only the first terms in a power series expansion in odd powers of  $T$ . The series is asymptotic, however, so that when the higher terms are appreciable ( $kT \sim e_F$ ), including them results in greater error. Stoner concluded that Equation (27) should be satisfactory as long as  $e_F > 2.6 kT$  and Equation (28) when  $e_F > 3.6 kT$ . Thus Equation (28) only holds when

$$-\frac{\partial e_F}{\partial T_e} < 39 \times 10^{-6} \text{ electron volts/}^\circ\text{K} \quad (29)$$

When more than one energy band is present at the Fermi level and when the density of states is not parabolic, Equations (25) and (26) are still valid because the Fermi energy of the metal must be the same for all energy bands and the total number of electrons in a system is fixed. Sun and Bend<sup>24</sup> and Wohlfarth<sup>25</sup> have treated the case of nickel assuming a parabolic density of states for electrons in the 4s band, and a parabolic density of holes of large effective mass in the 3d band. In this case the density of occupied states in the 3d band is very large and changes rapidly at the Fermi level. This can result in a large contribution to the temperature coefficient of work function. Equation (25) is then only valid below room temperature. In general high temperature predictions can be made in a graphical form by using tables of Fermi-Dirac integrals (see McDougal and Stoner<sup>26</sup>) in an approach similar to Wohlfarth's treatment of the case of nickel.

## The Effect of Atomic Vibrations on the Chemical Potential

Thermal vibrations of the nuclei in a metal should produce slight changes in the energy levels of the valence electrons. Herring and Nichols<sup>1</sup> have derived an expression for the change in the chemical potential utilizing the fact that

$$\left(\frac{\partial \mu}{\partial T}\right)_V = \left(\frac{\partial^2 F}{\partial T \partial Z}\right)_{V, W_1} = - \left(\frac{\partial S}{\partial Z}\right)_{V, T, W_1} \quad (30)$$

If a Debye model is assumed, the vibrational entropy  $S_V$  is

$$S_V = f(T/\theta) \quad (31)$$

$\theta$  is the Debye temperature. The entropy associated with the electronic specific heat has already been considered. Since  $\theta$  is a function of the elastic constants of a metal and these are partly determined by the kinetic energy and interaction energy of the valence electrons,  $\theta$  is a function of the number of valence electrons per atom. Calculating  $\frac{\partial S}{\partial Z} \frac{\partial Z}{\partial \theta}$  and  $\frac{\partial S}{\partial T}$  from Equation (31),  $\frac{\partial S}{\partial Z}$  can be eliminated from Equation (30). Then

$$\frac{\partial \phi}{\partial T_c} = - \left(\frac{\partial \mu}{\partial T}\right)_V = - \frac{\gamma_a}{\theta} \left(\frac{\partial \theta}{\partial Z}\right)_{V, W_1} \quad (32)$$

$\gamma_a$  is the specific heat per unit cell at constant volume, and  $\left(\frac{\partial \theta}{\partial Z}\right)_{V, W_1}$  is the change in  $\theta$  caused by adding a valence electron per unit cell and a compensating positive charge distribution to keep  $W_1$  constant. Herring and Nichols<sup>1</sup> stated that for transition metals this derivative

can be approximately determined by measuring the difference in Debye temperature between adjacent metals in the periodic table. Corrections for different atomic masses and volumes are small and can be determined using the theoretical expression for the Debye temperature:

$$\theta = \frac{V^{1/6} F(\sigma)}{M^{1/2} K^{1/2}} \quad (33)$$

M is the atomic mass, K the isothermal compressibility, and  $F(\sigma)$  a function of Poisson's ratio.

In the case of the monovalent metals, adding a valence electron and a positive charge at the nucleus forms a metal which has a much smaller lattice constant, a considerably different distribution of filled energy levels, and usually a different crystal structure. Thus the empirical approach proposed by Herring and Nichols for the transition metals should not be expected to be satisfactory for the monovalent metals. These metals can, however, be considered theoretically since adding a valence electron and a positive compensating charge to a metal will only change the Fermi kinetic energy and interaction energies of the electrons. The energy associated with the average coulomb field of the electrons and the ion-ion interactions must remain unchanged. Now

$$\frac{1}{K} = V \left( \frac{\partial^2 E}{\partial V^2} \right)_T \quad (34)$$

where E is the energy per unit cell of the crystal. If the variation of Poisson's ratio is neglected, differentiating Equations (33) and (34) with respect to Z, and employing the fact that

$$\mu = \left( \frac{\partial E}{\partial Z} \right)_{W_i, V} \quad (35)$$

then

$$\frac{\partial \phi}{\partial T_c} = - \frac{\gamma_a K V}{2} \left( \frac{\partial^2 \mu}{\partial V^2} \right)_T \quad (36)$$

Using the free electron approximation for  $\mu$ ,

$$\mu = e_f + E_f + E_{cm} \quad (37)$$

$$\frac{\partial \phi}{\partial T_c} = - \frac{\gamma_a K}{9V} (5 e_f + 2 E_f + V'_c) \quad (38)$$

where

$$V'_c = \frac{E_c r_s}{r_s + 5.1 a_h} \left[ \frac{2}{3} + \frac{r_s}{r_s + 5.1 a_h} + \frac{r_s^2}{(r_s + 5.1 a_h)^2} \right] \quad (39)$$

The term due to the correlation energy is small in comparison with the effect of the exchange or Fermi energy for any value of  $r_s$  due to the small curvature of the  $E_c - r_s$  relationship.

It should be expected that  $\partial \phi / \partial T_c$  would vary considerably with temperature since  $\gamma_a$  and  $K$  are temperature dependent. The effect of thermal expansion should also vary since  $\alpha$  is temperature dependent. Considerable variations in  $d\phi/dT$  might then be expected to occur. The two effects are, however, of opposite sign and will thus tend to cancel. In addition the two effects are intimately related since Gruneisen's law requires that

$$\alpha = \frac{\gamma_g}{3} \frac{\gamma_a K}{V} \quad (40)$$

where  $\gamma_g$  is a constant. The sum of the two effects can then be expressed in the form

$$\frac{\partial \phi}{\partial V} \frac{dV}{dT} + \frac{\partial \phi}{\partial T_c} = \frac{\partial \phi}{\partial V} \frac{dV}{dT} (1 - \gamma_T / \gamma_g) \quad (41)$$

where

$$\gamma_T = \frac{V \left( \frac{\partial^2 \phi}{\partial V^2} \right)_T}{2 \frac{\partial \phi}{\partial V}} \quad (42)$$

is only slightly temperature dependent.

$$\gamma_T = \frac{5e_F + 2E_F + V_c'}{3(e_F + V_c - \phi)} \quad (43)$$

when the free electron approximation holds.

Calculations for several monovalent metals show that the two effects cancel almost exactly because  $\gamma_g$  and  $\gamma_T$  are very nearly equal. The cancellation cannot be expected to be exact since different crystal faces have slightly different temperature coefficients. Table I lists values of  $\gamma_g$  obtained from several methods (see Reference 27). The average of these values in each case is quite close to  $\gamma_T$ , although the monovalent noble metals do not agree as closely as the alkali metals.

Table II lists the contributions to  $d\phi/dT$  which have been considered up to this point. Comparing the second and third columns it is apparent that the cancellation of the two large effects is accurate to a few microvolts per degree. The last column listing the effect of the electronic specific heat is also very small. The second to last column was inserted to show the importance of the correlation energy in

TABLE I  
Values of  $\gamma_g$ ,  $\gamma_T$

Element	Vapour Pressure and Compressibility	Change of Compressibility with Volume	Direct Calculations	Average	$\gamma_T$
Li	1.55	0.63	1.17	1.12	1.17
Na	1.58	1.83	1.25	1.55	1.53
K	1.53	2.55	1.34	1.81	1.85
Cu	2.13	1.9	1.96	2.00	2.20
Ag	2.33	2.5	2.40	2.41	2.72
Au	2.60	---	3.03	2.82	2.58

TABLE II  
Contributions to  $\frac{d\phi}{dT}$

Element	$\frac{\partial \phi}{\partial V} \frac{dV}{dT}$ (300°K)	$\frac{\partial \phi}{\partial V} \frac{dV}{dT} (1 - \gamma_T/\gamma_g)$	20 percent $E_c$ Term	$\frac{\partial \phi}{\partial T_e}$
$10^{-6}$ Electron Volts/°K				
Li	74	-3	10	1.2
Na	123	2	11	1.2
K	156	-3	11	1.0
Cu	55	-6	3	0.8
Ag	36	-5	3	0.7
Au	30	3	2	0.7

determining  $d\phi/dT$ . The figure quoted in this column is the uncertainty due to the estimated possible error in Wigner's theoretical calculation.

The contributions thus far investigated cannot explain any large temperature coefficient of the work function. The only contribution which remains to be considered is the electrostatic effect of ion core vibrations.

#### The Electrostatic Effect of Thermal Vibrations at Constant Volume

Herring and Nichols<sup>1</sup> have postulated that atomic vibrations at constant volume can change the average electrostatic potential in a crystal by moving the ion cores of the atoms from their equilibrium positions. Averaged over a large number of cells these motions produce a mean effect like that of a lattice of symmetrically extended ion charge clouds. It was shown that the change in the average internal electrostatic potential energy of an electron due to a change in charge density is

$$\Delta W_i = - \frac{2\pi e}{3V} \int_V r^2 \Delta \rho \, dV \quad (44)$$

where  $V$  is the volume of the unit cell,  $\Delta \rho$  is the change in charge density at a distance  $r$  from the origin, and  $dV$  is an element of volume at  $r$ . This derivation is based on the assumption that the unit cell is electrically neutral and has been chosen to have zero dipole moment.

Equation (44) was applied in the idealized case of a monatomic lattice obeying Debye's theory of specific heat. It was assumed that changes in the charge density of the free electrons were negligible and that the bound electrons and the nuclei vibrated like rigid ions having

a charge  $Z_e$ . These are rough approximations even for alkali metals, for the effective vibrating charge can be considerably different. Since the treatment given by Herring and Nichols is very brief and only states the results for temperatures well above the Debye temperature, a more complete derivation follows.

The energy associated with thermal excitation is present in a metal in the form of phonons of vibrational energy, each phonon having an energy  $hf$  where  $h$  is Planck's constant and  $f$  the vibrational frequency. If the energy of a phonon is used to vibrate one ion core, the motion of the core will be simple harmonic with a mean square ion displacement

$$r_f^2 = h/4\pi^2 Mf \quad (45)$$

where  $M$  is the mass of the ion core. The total mean square vibration of any core is the sum of the mean squares of the vibrations caused by all the phonons present. In a metal the distribution of vibrational frequencies is in principle discrete, but the separation of the vibration frequencies is so small that the spectrum can be considered continuous. The Debye form for the number of allowed frequencies per ion core in the frequency range  $df$  is

$$g(f)df = 9f^2(h/k\theta)^3 df \quad (46)$$

when  $hf \leq k\theta$ . When  $hf > k\theta$ ,  $g(f) = 0$ .  $\theta$  is the Debye temperature. The average number of phonons of frequency  $f$  is  $1/(-1 + \exp hf/kT)$ , so the total mean square displacement of an ion core is

$$R^2 = \int_0^{(k\theta)/h} \frac{r_f^2 g(f) df}{-1 + \exp hf/kT} = \frac{9h^2 T^2}{4\pi^2 M k \theta^3} \int_0^{\theta/T} \frac{x dx}{\exp x - 1} \quad (47)$$

Differentiating Equations (44) and (47) with respect to T,

$$(\Delta W_i = -\frac{2\pi}{3V} Ze^2 R^2)$$

$$\frac{\partial W_i}{\partial T} = \frac{3h^2 Ze^2 T}{2\pi V M k \theta^3} \int_0^{\theta/T} \frac{x^2 \exp x dx}{(1 - \exp x)^2} \quad (48)$$

For any temperature the integral can be expanded in a power series in  $\exp(-x)$  and integrated term by term, but for temperatures of the order of, or greater than  $\theta$ , a series expansion in powers of  $x$  is simpler and more rapidly convergent. The following expansions are accurate to approximately one percent:

when  $T \gg \theta/2$ ,

$$\frac{\partial W_i}{\partial T} = \frac{\partial W_i}{\partial T_m} (1 - (\theta/6T)^2) \quad (49)$$

and when  $T < \theta/7$ ,

$$\frac{\partial W_i}{\partial T} = \frac{\pi^2 T}{3\pi} \frac{\partial W_i}{\partial T_m} \quad (50)$$

$$\frac{\partial W_i}{\partial T_m} = \frac{3h^2 Ze^2}{4\pi V M k \theta^2} = \frac{1.26 \times 10^4 Z}{V M \theta^2} \text{ electron volts/}^\circ\text{K} \quad (51)$$

when  $V$  is in cubic angstroms,  $M$  in atomic units, and  $\theta$  in degrees Kelvin. Note that Equation(50) satisfies the requirement that

$$\frac{\partial W_i}{\partial T} \rightarrow 0 \quad \text{as } T \rightarrow 0 \quad (52)$$

The above derivation has neglected two effects arising from distortion of the electron charge distribution. The valence electron distribution is not exactly uniform throughout any metal. Near the nuclei some variations in charge density exist. Since the electron motions are much more rapid than thermal vibrations, these variations in charge density will accompany the nuclei. Thus the effective value  $Z'$  of the vibrating charge will be less than  $Z$  if the electron charge density is greater near the nuclei than the average charge density throughout the metal. The other factor to be considered is that the outer shells of the ion cores in some cases are comparable in diameter to the dimensions of the unit cell, particularly in the case of newly completed  $d$  shells. These outer shells can be expected to be restricted in their motion because of the proximity of the neighbouring ion cores. This effect will tend to increase the size of the vibrating charge.

The electrostatic effect of thermal vibrations should thus be negative in sign, but the effective value of the vibrating charge is in doubt.

#### Theoretical Results

The contributions to the temperature dependence of the work function can now be written in the form

$$\frac{d\phi}{dT} = \frac{\partial \phi}{\partial V} \frac{dV}{dT} \left(1 - \frac{\gamma_T}{\gamma_g}\right) + \frac{\partial \phi}{\partial T_e} - \frac{\partial W_i}{\partial T} \quad (53)$$

In the case of the monovalent metals the last contribution is much greater than the effects of all the other contributions. This is apparent from the results shown in Table III. The assumption that  $Z' = 1$  should give the order of magnitude of the temperature coefficient.

This theoretical development can be checked in three separate ways. The order of magnitude of experimental temperature coefficients is a first check on the theory. This result can be considered as establishing  $Z'$ , since this is a parameter which is not known exactly. Presuming the order of magnitude is predicted by the theory, a further experimental check is possible. If a thermal expansion effect were chiefly responsible for the temperature coefficient,  $d\phi/dT$  should differ appreciably at different temperatures since the expansion coefficient of a metal is not uniform over large ranges of temperature. A temperature coefficient due to the ion core vibrations, however, should vary only slightly at temperatures above the Debye temperature. This type of check is only possible on metals having large temperature coefficients and with an experimental method capable of high accuracy. The third experimental check is essentially a check of Smoluchowski's theory of the surface dipole layer. This check consists of comparing the temperature coefficients of different crystal faces of the same metal.

The author's chief contribution to the theory consists of showing that the effect of thermal expansion is cancelled by the effect of thermal vibrations on the chemical potential. In the case of the thermal expansion effect the relationship of the author's result to those of Wigner and Seely has been stated. Beyond the point of relating  $d\phi/dT_c$  and  $\partial\phi/\partial Z$  (Equation (32)), the effect of thermal excitation on the chemical potential has never been previously considered theoretically. Thus the cancellation of the two effects has not been previously

TABLE III  
Theoretical Results

Metal (300°K)	$\frac{d\phi}{dT}$ ( $Z' = 0$ )	$\frac{d\phi}{dT}$ ( $Z' = 1$ )
$10^{-5}$ Electron Volts/°K		
Li	-0.2	-45
Na	0.3	-60
K	-0.2	-44
Cu	-0.5	-17
Ag	-0.4	-15
Au	0.4	-13

TABLE IV  
Data for Calculating  $\frac{d\phi}{dT}$

Element	$\theta$ °K	$\alpha$ $10^{-6}/\text{°K}$	$r_s$ $\frac{\circ}{\text{Å}}$	$m/m^*$	$\phi$ eV
Li	423	56	1.72	0.653	2.48
Na	152	71.5	2.11	1.069	2.28
K	100	83	2.60	1.72	2.22
Cu	318	16.3	1.41	1	4.50
Ag	215	18.5	1.59	1	4.31
Au	170	14.3	1.58	1	4.25
References:	16	28	29	16	30, 31

predicted, and the result which follows has never been postulated: a Debye model for the ion core vibrations can then predict the form of the chief contribution to the temperature dependence of the work function.

## EXPERIMENTAL MEASUREMENTS ON THE MONOVALENT NOBLE METALS

## Introduction

The temperature dependence of the work functions of only a very few metals has been investigated. Tungsten has been studied the most frequently. Kruger and Stabenow<sup>32</sup> used the cooling effect of electron emission to measure the work function of tungsten at different temperatures. The experimental temperature coefficient was  $6 \times 10^{-5}$  eV/°K over the temperature range 2100-2700 °K. These measurements were taken at pressures of the order of  $10^{-6}$  millimeters of mercury, hence were subject to the possibility of very rapid contamination. Langmuir<sup>35</sup> and Potter<sup>9</sup> also investigated tungsten, the former by measuring the shift in diode characteristics when the anode was heated, and the latter by a capacitive contact potential method. Their results over the temperature range 300°K to 1000°K were  $-55 \times 10^{-6}$  eV/°K and  $63 \times 10^{-6}$  eV/°K respectively. In both cases contamination effects were observed.

Tantalum was investigated by Kruger and Stabenow at the same time as tungsten and the same temperature coefficient observed. Photoelectric measurements by Cardwell<sup>34</sup> gave qualitatively the same temperature coefficient at low temperatures.

Palladium was carefully investigated by DuBridg and Roehr<sup>35</sup> using a Fowler plot to measure the photoelectric work function. The accuracy of the measurements was sufficient to show that the temperature coefficient was of the order of  $1 \times 10^{-5}$  eV/°K over the range 300°K to 1000°K. The results in this case were taken in a very good vacuum, but preparing the surface solely by bakeout could not guarantee that the surface of the metal was clean.

Photoelectric measurements on several other metals have been

taken, but the accuracy of the results and the fact that measurements were not taken at a sufficiently large number of temperatures makes it impossible to deduce even the sign of the temperature dependence with any certainty. In general the photoelectric method is not satisfactory for measuring the temperature dependence because considerable time is required to record the data for a Fowler plot. Thus if a clean surface is prepared in a vacuum, the surface is liable to become contaminated before a complete set of results is obtained. The problem of contamination will be discussed more fully in a later section.

#### Experimental Method

The method chosen for investigating the temperature coefficient of work function involved measuring the temperature dependence of the contact potential between two metal surfaces. In the absence of other electric fields, when two surfaces are at temperatures  $T_1$  and  $T_2$ , the potential of surface 2 with respect to surface 1 is

$$V_{21} = (\phi_1 - \phi_2)/e + \int_{T_1}^{T_2} \xi \, dT \quad (54)$$

where  $\phi_1$  and  $\phi_2$  are the work functions of the two surfaces, and  $\xi$  is the absolute thermoelectric power of the metal joining them (Reference 36).

Thus

$$\frac{d\phi_2}{dT} = e \left[ \xi - \frac{dV_{21}}{dT} \right] \quad (55)$$

when surface 1 is kept at a constant temperature. In most cases the

absolute thermoelectric power is a small correction of the order of a few microvolts per degree Kelvin.

One of the most important reasons for the choice of a capacitive contact potential method is the fact that when the work function of a surface is not constant as is the case with contaminated or polycrystalline metal surfaces, the work function measured is the arithmetical mean work function. The explanation of this fact lies in the mechanism of detecting a contact potential difference.

A contact potential difference exists between two electrically connected metal surfaces because it is necessary for equilibrium between the two metals. This potential difference is produced by the transfer of charge from one metal to the surface of the other. If the capacitance between the two surfaces is  $C$ , the equilibrium charge on this condenser is  $q = CV_{21}$ . If one of the surfaces is moved, a different charge must reside on the condenser because  $C$  is altered. The resultant flow of charge makes it possible to detect a contact potential difference. When the work functions are not uniform over the surfaces involved, the situation is somewhat more complicated. If the areas of non-uniformity are evenly spread over the surfaces and the dimensions of these areas are small in comparison with the distance separating the surfaces, each element of surface area then sees the other surface as an effective equipotential. The charge residing on such an element is determined by its work function, and the total charge on the condenser is

$$q = \int_1 \frac{(\phi - \phi_2)}{e} dC = \int_2 \frac{(\phi_1 - \phi)}{e} dC \quad (56)$$

The effective work functions of the two surfaces are then

$$\phi_1 = \frac{1}{C} \int_1 \phi dC \quad \text{and} \quad \phi_2 = \frac{1}{C} \int_2 \phi dC \quad (57)$$

If the temperature of a surface is increased, unless the geometry of the system alters radically, the weight of each portion of the surface will remain constant, and a temperature coefficient of work function can only be observed when the work function of the heated surface alters.

The arithmetical mean work function is not measured by a method requiring the photoelectric or thermionic emission of electrons. If any variations in work function exist over the emitting surface, the various portions of the surface are weighted exponentially according to their work functions in determining the number of electrons emitted. Thus the effective work function of a non-uniform emitting surface can be very different from the arithmetical mean. The weighting of the areas of different work functions also varies with the temperature; in fact a temperature coefficient of the effective work function of the order of  $10^{-4}$  eV/°K can be measured, even when no variation exists in the actual work function. Thus emission methods can give misleading temperature coefficients when using a polycrystalline surface, even if the surface is clean. Similar effects exist when the retarding potential characteristic of a diode is used to follow changes in the anode work function. These effects are discussed in detail in References 1 and 30. A capacitive contact potential method is therefore preferable for studying the temperature dependence of the average work function of a contaminated or clean polycrystalline surface.

Two different methods of varying the capacitance were studied.

One method attempted used a perforated disk rotating beside a smaller fixed plate. The final method used a vibrating condenser plate.

The rotating disk is shown in Figure 1. It was driven by an induction motor consisting of a nickel wire cage and the stator of a phonograph motor. Two fixed condenser plates were used. One was kept at a high potential to provide a reference voltage for a synchronous detector, and the other served as the test surface. This arrangement was satisfactory at high pressures and could be used to measure contact potentials to an accuracy of about two millivolts. At pressures between  $10^{-7}$  and  $10^{-8}$  millimeters, increased difficulty was experienced, particularly after bakeout. Increased friction at the bearing surfaces produced more noise as the surfaces became clearer, and decreased the accuracy to the point where the method could not be used. Lubrication with aquadag was attempted but was not satisfactory.

A vibrating condenser was used in the final measurements. This method avoided the problem of friction found in the above method and was also preferable because less metal was involved in the tube construction. The problems of outgassing were thus decreased.

Two views of the vibrating condenser are shown in Figures 2 and 3. The vibrator was made in two parts: a heavy 0.060" tungsten support sealed through a nonex pinch, and a light 0.030" extension carrying the vibrating condenser plate. The plate was made of 0.005" nickel sheet to keep the vibrator load as light as possible. The two portions of the vibrator were held together by a piece of heavy nickel sheet (about 0.030") which was also used to excite the vibrator magnetically. This arrangement had a relatively high resonant frequency characteristic mainly of the heavy support. The resonant frequency of the light rod and condenser

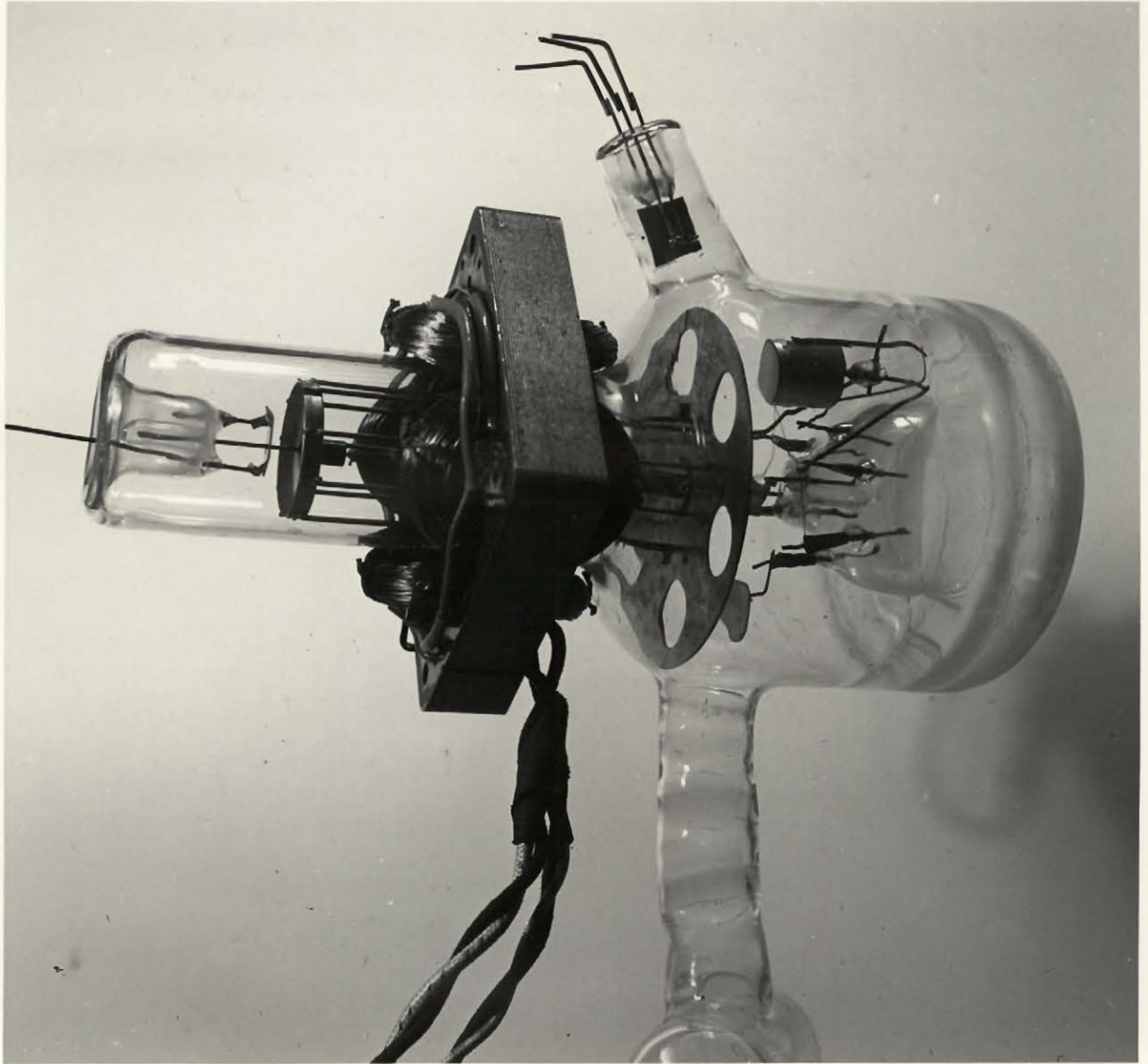


Figure 1 - Rotating Disk

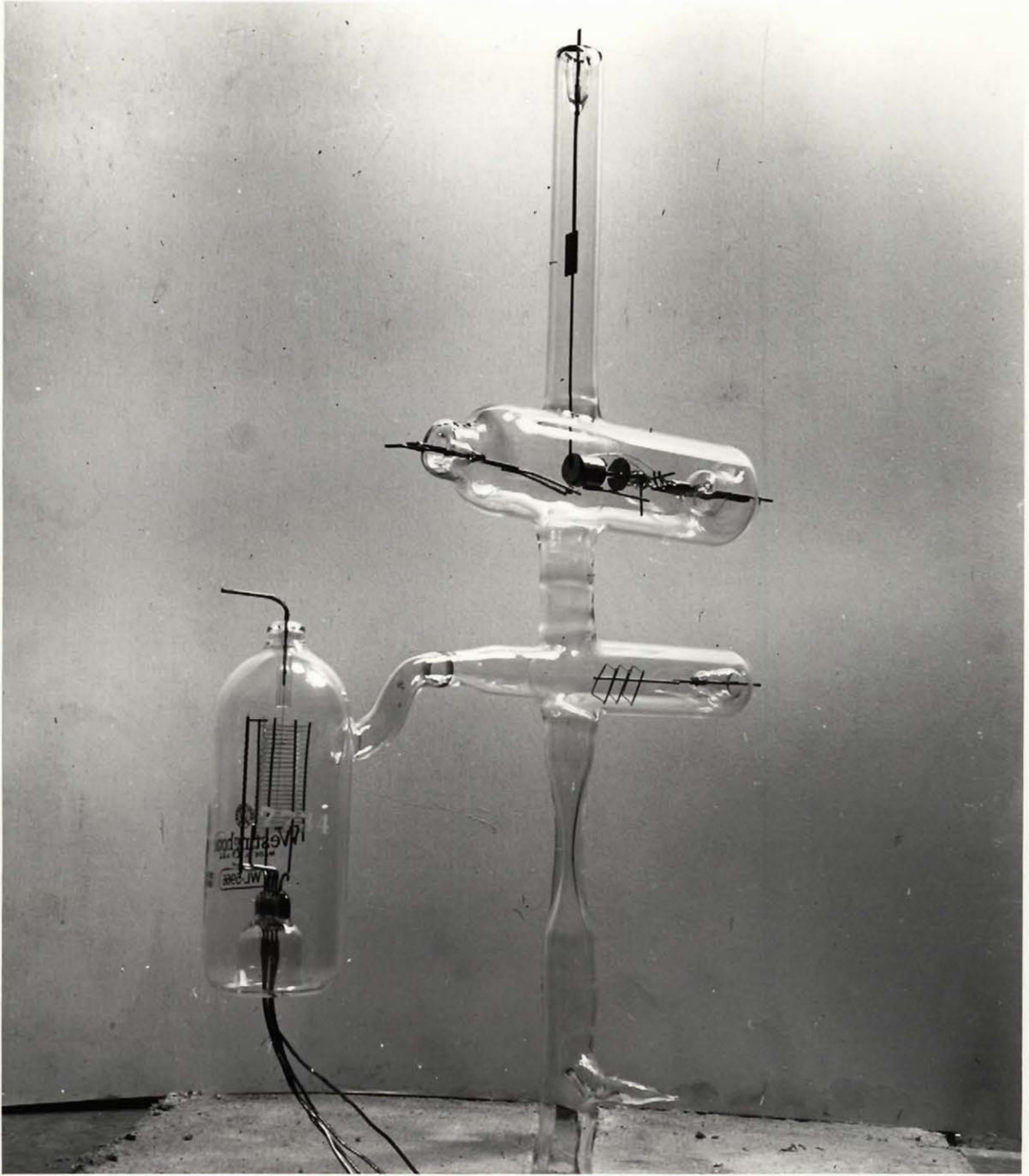


Figure 2 - Vibrating Condenser

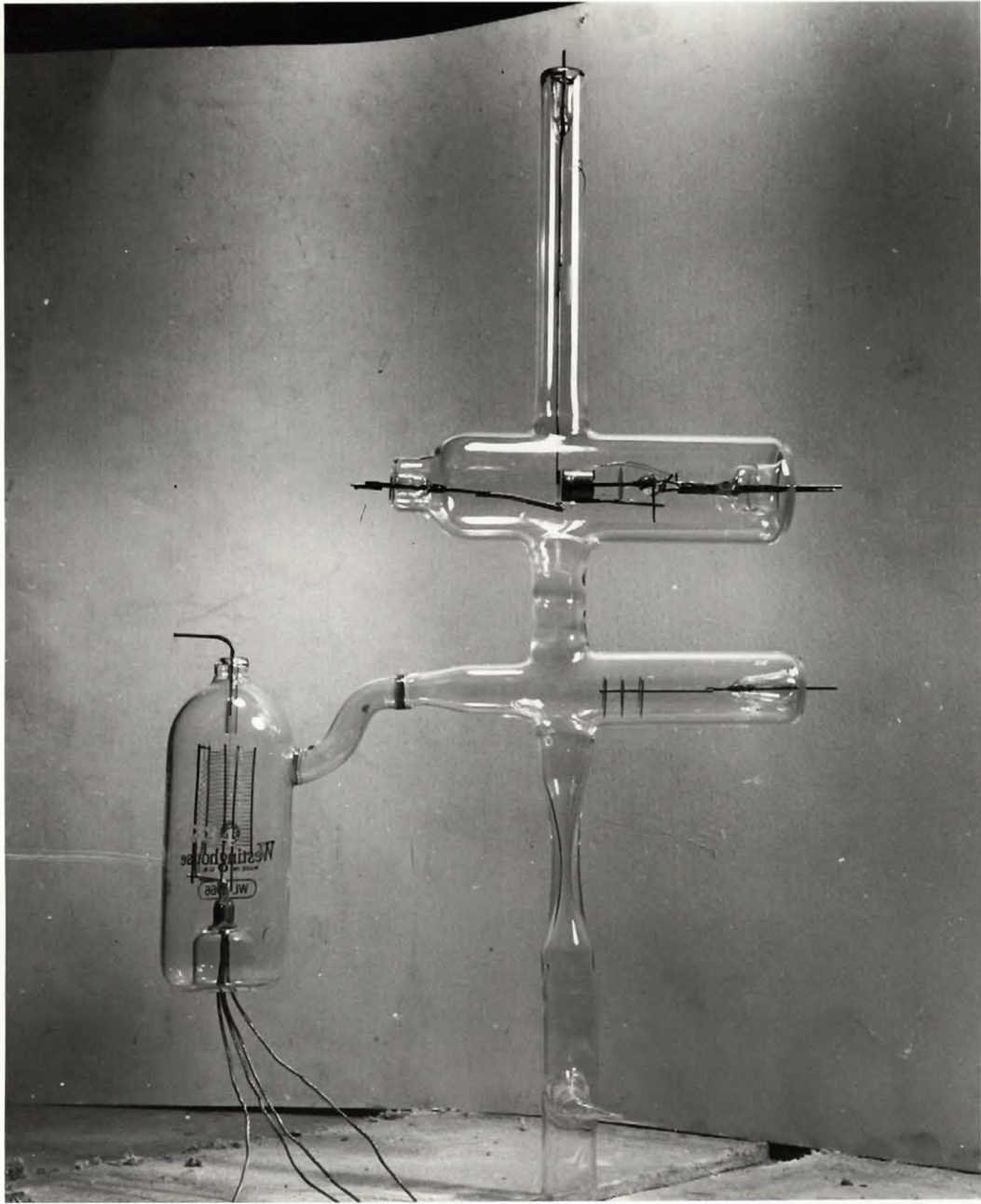


Figure 3 - Vibrating Condenser

plate was adjusted so that with a given excitation the condenser plate had a maximum amplitude of vibration at resonance. The net result was a vibrator having a higher resonant frequency and larger amplitude of vibration than could be obtained with a simple vibrator and the same means of excitation. The resonant frequency was approximately 40 c.p.s. for the two similar tubes used in making the experimental measurements.

The fixed condenser plate and its heater were constructed as a sub-assembly. The fixed plate was a spun 0.010" nickel cap fitting a 5/8" diameter nickel tube. A Pt -Pt 10 percent Rh thermocouple was spot-welded to the outside of the nickel cylinder. The heater, a helix of 0.010" tungsten wire coated with alundum, was mounted inside the cylinder. To avoid sag, heater supports (0.040" tungsten) much heavier than the heater wire were used. These were held in position by a nonex bead. The bead also contained a lead to support the fixed condenser plate. This fixed the relative positions of the heater and the cylinder, and maintained a high leakage impedance between them. The alundum heater coating was necessary to prevent shorts between turns of the heater coil. The sub-assembly was completed by the addition of two nickel shields. A heat shield across the open end of the cylinder virtually enclosed the heater, and a second shield was added to protect the nonex bead from radiated heat and evaporated metal. The sub-assembly was then mounted on a nonex pinch containing four 0.060" tungsten leads, two for the heater current and two for the thermocouple leads. Small nickel shields on each of these leads assured freedom from leakage caused by evaporated metal.

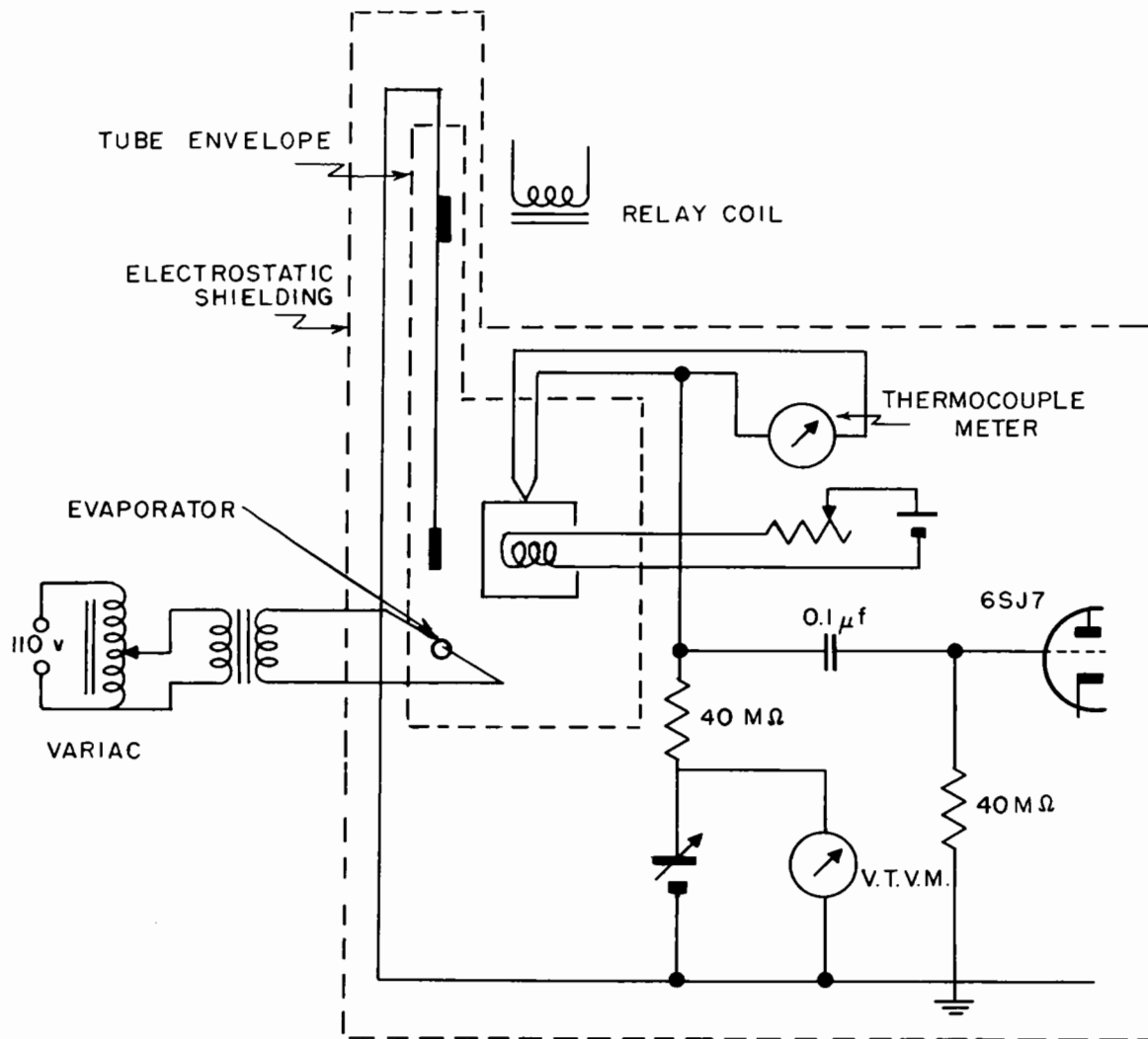
An evaporator was used to deposit metal films on the condenser plates. This was a pure metal bead fused in a tungsten basket. The bead was mounted below the condenser in a position where it could evaporate

metal on both condenser plates but not on the thermocouple junction. Since some portions of the cylinder could not be covered by evaporation, the vibrating plate was made slightly smaller than the fixed plate to eliminate capacitive coupling to the sides of the cylinder. To ensure adequate coverage over the end of the cylinder, the bead was placed as close to the condenser as possible. All the beads used were fused and outgassed before assembly. With sufficient heating they could be made to wet a tungsten basket and the leads to it. This ensured that evaporation occurred only from the metal of the bead. Since most of the evaporation occurred from the points at which the heater current entered and left the basket, the position of the bead was adjusted accordingly. The evaporator design was essentially the same for copper, silver, and gold, but 0.015" instead of 0.010" tungsten wire was necessary for the basket in the case of gold. The nickel supports carrying the heater current were also heavier in this case. The metals used in forming the beads were high-conductivity oxygen-free copper (99.75 percent), electrolytically pure silver (99.99 percent) and a gold sample of 99.9 percent guaranteed purity.

A side tube containing several K.I.C. barium getters and a commercial ionization gauge, a Westinghouse WL 5966, of the Bayard-Alpert type were the other essential portions of the sealed-off system.

The tube envelope was of pyrex with nonex seals wherever tungsten leads were necessary. The assembly of the tube parts was not critical since only a simple glass-blowing operation was needed to adjust the positions of the evaporator and the two condenser plates.

Figure 4 is a schematic diagram of the vibrating condenser circuit, Figure 5 a block diagram of the complete system, and Figure 6



SCHEMATIC DIAGRAM OF EXPERIMENTAL SETUP

Figure 4

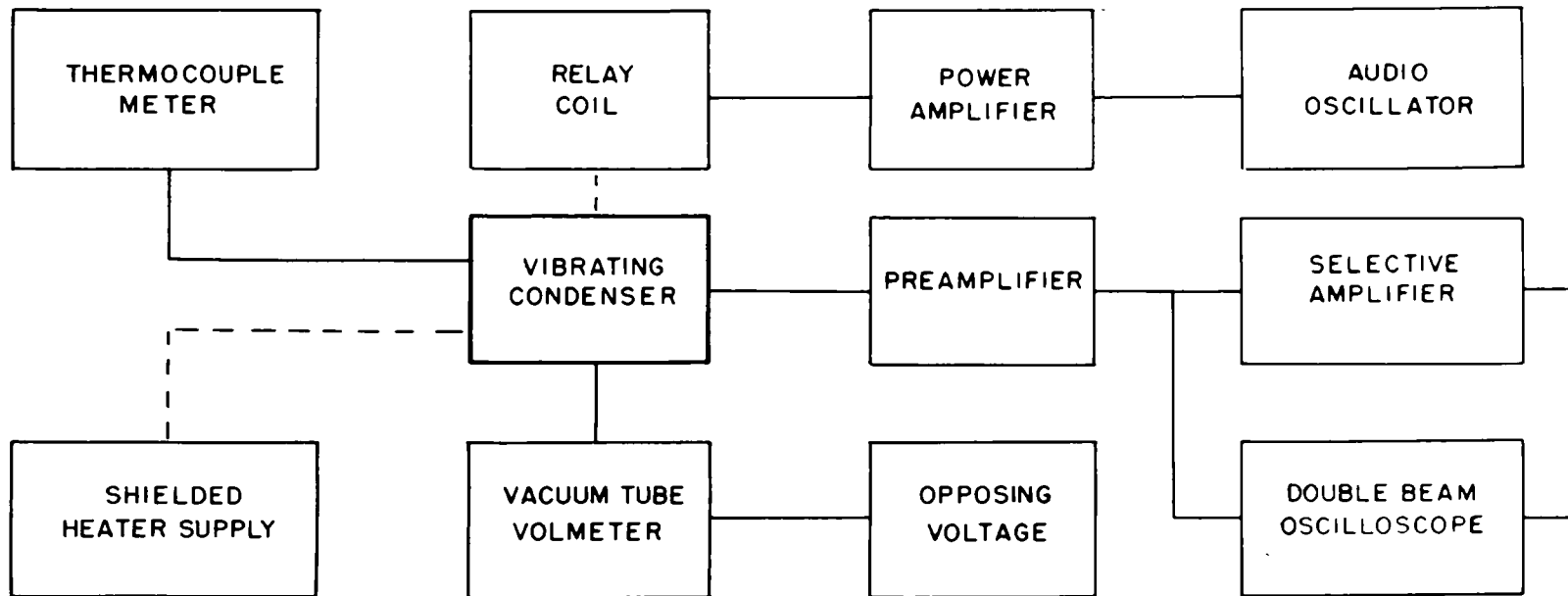


FIG. 5 BLOCK DIAGRAM OF APPARATUS

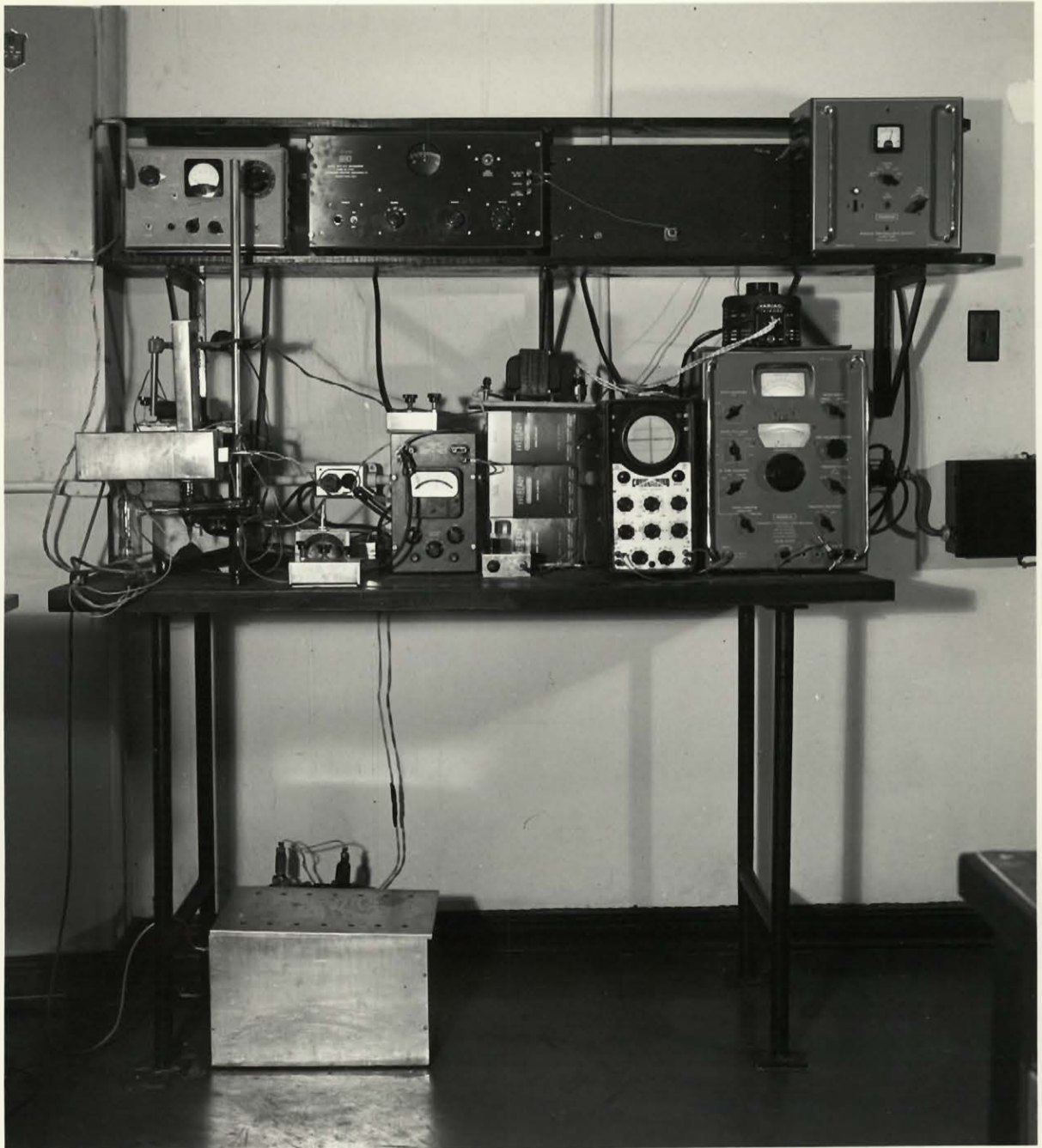


Figure 6 - Experimental Arrangement

a photograph of the final set-up.

The response of the system to a direct voltage in the vibrating condenser circuit is treated in Appendix I. The results of the discussion can be summarized by stating that when the vibrator is operating, an alternating voltage proportional to the direct e.m.f. in the circuit appears across the resistor connecting the two condenser plates, and that while stray capacity decreases the sensitivity of the circuit, it does not affect the signal-to-noise ratio because the stray capacity shunts the noise equally effectively. The choice of circuit parameters predicts a ratio of signal voltage to r.m.s. noise voltage of approximately unity when the direct voltage unbalance in the condenser circuit is of the order of one millivolt.

In the experimental set-up the alternating voltage was amplified by a conventional battery operated preamplifier. The only unusual care taken was in the choice of a low noise and low grid current 6SJ7 for the input tube. This was necessary because a 40-megohm grid leak resistor was used. The preamplifier output was fed into a selective amplifier. This was a Muirhead Pametrada Wave Analyser. The filtered output was displayed using one beam of a Cossor double-beam oscilloscope. To aid in setting up the system the analyser input voltage was displayed using the other beam.

The source of voltage opposing the contact potential was a potentiometer circuit. The voltage inserted in the condenser circuit could be read to one millivolt by a General Radio vacuum-tube voltmeter.

The vibrator was excited at its resonant frequency by a relay coil. The power was supplied from a power amplifier driven by a stable oscillator. To isolate the two circuits, the oscillator frequency used was half the resonant frequency of the vibrator. A condenser was placed

across the relay coil to resonate it at the oscillator frequency. This helped to eliminate distortion and subsequent pickup of harmonics. The distortion was present because the power amplifier, a transformer-coupled device, was forced to operate at 20 cycles per second, which was below its normal low frequency limit.

Since the circuit containing the vibrating condenser formed a high impedance input circuit, and low level detection was required, it was necessary to shield the tube. Electrostatic shields enclosed the part of the tube containing the condenser, the thermocouple meter and the heater supply for the fixed condenser plate. The relay coil excited the vibrator through the shield. It was necessary, however, to mount the coil as close to the vibrator as possible to achieve strong enough coupling. The thermocouple meter was a 55-ohm, 200-microampere moving-coil galvanometer.

A d-c supply was used for the heater of the fixed condenser plate. When the heater circuit was connected to ground, the leakage resistance of the nonex bead holding the heater and fixed plate was not large enough at high temperatures. Appreciable current from the heater supply could then be coupled through the resistor in the circuit containing the vibrating condenser. Floating the heater circuit eliminated this current and also ensured that no appreciable emission could be drawn from the heater.

#### Vacuum Procedure

The preparation and maintenance of clean surfaces is a problem equal in importance to that of measuring the properties of these surfaces. A monolayer of adsorbed gas can considerably alter the work function of a

surface as can impurities and other surface contaminants. The time for deposition of a monolayer of contaminating gas on a clean surface is also very short except in very high vacua. The order of magnitude of the pressure restriction is discussed in Appendix II from which it can be concluded that at pressures below  $10^{-8}$  millimeters of mercury it is possible to make rapid measurements of surface properties under conditions where the progress of a contamination process can be observed. In this pressure range the best criterion for the reliability of results is their reproducibility and freedom from drift.

Two methods have been used to prepare clean surfaces in a vacuum. Surfaces of the most refractory metals have been outgassed and cleaned simply by heating them to a very high temperature. This breaks down surface oxides and drives off other impurities and adsorbed gases. The more volatile metals, however, evaporate more rapidly than many of their impurities, hence preparation of a clean surface by this method is impossible. The evaporated metal on the other hand is purified by fractional distillation. Thus if enough of the metal is evaporated on a surface to form a thick film, a clean surface of the pure metal can be produced. This film must of course be deposited under stringent vacuum conditions to avoid contamination.

Since the experimental work was done using intermediate melting point metals, the evaporation technique for producing clean surfaces was preferable to depending solely on outgassing for long periods. In preparing the experimental set-up, however, the assembly and bake-out schedule were still designed to effect a maximum of outgassing of the tube parts and to produce as good a vacuum as possible.

Prior to assembly, the tube parts and tube envelope were given

a thorough solvent degreasing in acetone, trichlorethylene and methyl alcohol. Immediately after assembly the tube was sealed on a pumping system and checked for leaks. The pumping system consisted of a Cenco Megavac forepump, a Distillation Products three-stage fractionating oil diffusion pump with water cooling, and two liquid air traps in the high vacuum line. The diffusion pump fluid was D.C.702. Separate ovens were provided to bake out the cold traps and the tube.

The bake-out schedule was conducted in 24-hour cycles. The cold traps and tube were baked for an initial period of two to three hours, the cold traps at 250°C and the tube at 450°C. After this interval the oven around the cold traps was turned off and the temperature of the other oven lowered to about 430°C. Previous to this, after the first hour of bake-out, power was applied to the heater of the fixed condenser plate and the nickel cylinder raised to a temperature of 850°C. The fused metal bead was also heated to about the same temperature. The heating of these parts was continued for the remainder of the bake-out period. When the cold traps had cooled to room temperature, liquid nitrogen was applied to the trap nearest the diffusion pump. To avoid the problem of maintaining a constant level of coolant, the trap was only partially immersed in the liquid nitrogen and the coolant flask raised a small amount at roughly half-hour intervals. When the first trap was completely immersed, the same procedure was followed with the second trap.

After about six hours bake-out the oven heat was turned off and the ionization gauge out-gassed by electron bombardment until the oven was cool. In two hours the oven temperature dropped to about 50°C and the oven was raised. The getters were then out-gassed for several minutes using radio-frequency heating. The metal bead was melted and cooled several times to get rid of absorbed gas. An appreciable amount of metal

was evaporated in this process.

This cycle was repeated for three consecutive days, resulting in approximately a tenfold decrease in ultimate pressure each day. The following conditions were satisfied when the system was considered ready for seal-off. The ionization gauge reading was of the order of  $10^{-9}$  millimeters with the tube cold, and no increase was observed when the fixed condenser plate was raised to  $600^{\circ}\text{C}$ . The metal bead could be raised to evaporating temperature and cooled without affecting the ultimate pressure, and the getters likewise did not produce more than a transient pressure change when heated and cooled. The getters were then fired and the tube sealed off. During the sealing-off process the ion gauge readings did not exceed  $10^{-7}$  millimeters, and after completion of the operation the pressure dropped to about  $10^{-9}$  millimeters. The ultimate pressure could not be measured accurately since a pressure of  $1 \times 10^{-9}$  millimeters corresponded to a deflection of 1/200th of full scale on the most sensitive range of the ion gauge control unit.

#### Measurements

The procedure followed in taking measurements was similar in every case. Before evaporating a film, the frequency and amplitude of the oscillator were adjusted until the vibrator was moving with a large amplitude at its resonant frequency. The tuned amplifier was then adjusted for maximum output and the fixed plate heated to  $500^{\circ}\text{C}$ . Several readings were taken to check the operation of the circuits. The evaporator was then heated until a film was deposited rapidly. Since the behaviour of the system was somewhat different in the case of each metal, the three metals examined will be discussed separately.

After sealing off the system and before depositing a new film, an examination was made of the silver film deposited during the out-gassing cycles, and subject to contamination during the sealing-off process. The measurements were unstable at temperatures above 400°C, but below 400°C a value of  $-(dV_{21})/(dT)$  of -3 microvolts per degree Kelvin was measured. Essentially the same behaviour was observed with films of copper and gold deposited under the same conditions. Measurements taken with the rotating disk arrangement yielded values of  $0 \pm 2$  microvolts per degree Kelvin for an out-gassed nickel surface at pressures below  $10^{-8}$  millimeters of mercury, in a dynamic system.

The properties of films deposited after seal-off were very different from those of the films deposited before. The measurements on silver films will be discussed first.

After one or two minutes of evaporation, a few contact potential readings were taken. The evaporation was then resumed for a short time. The maximum pressure indicated by the ion gauge during the evaporation was  $6 \times 10^{-9}$  millimeters of mercury, but the pressure dropped rapidly when the evaporation was stopped. The contact potential reached a stable value after the first film. Measurements were started within a minute of the time evaporation ceased. One of the films was cooled and heated through three cycles. The time occupied by these cycles was varied between ten and forty-five minutes. No drift in contact potential was observed over a period of three hours. The results shown in Figure 7 were obtained from successively deposited films.

The pressure rise measured during the process of evaporation was almost certainly due to out-gassing of the bead. The probability of an atom of evaporated metal sticking to a cold surface is practically unity, hence the probability of an atom of evaporated metal undergoing

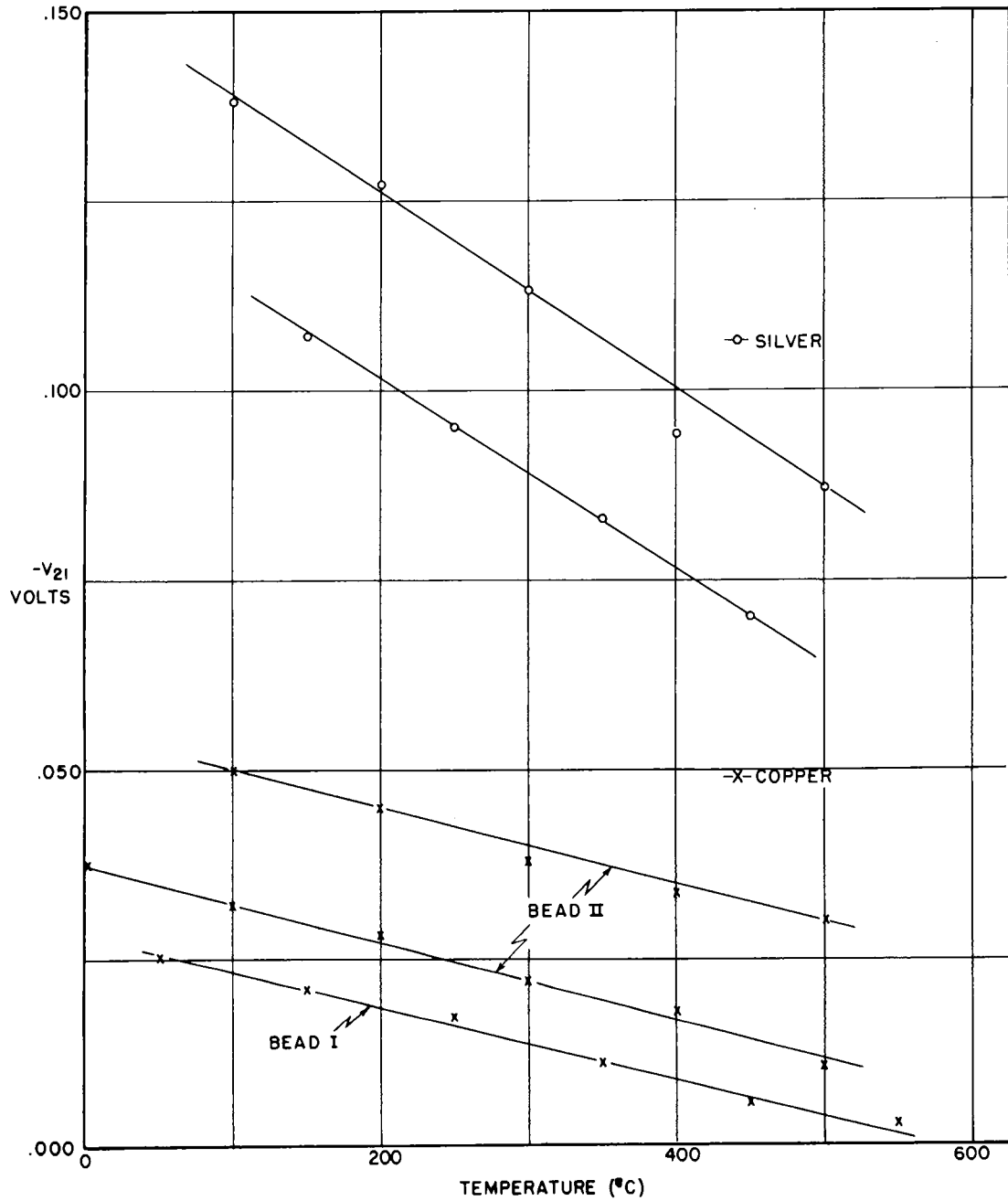


Figure 7 - Results from Silver and Copper

the multiple collisions necessary to reach the ion gauge is extremely small. Judging by the temperature of the evaporator, the vapour pressure of the silver bead during the evaporation was at least  $10^{-2}$  millimeters, hence the contamination represented by the ion gauge pressure reading was probably slight. This was also borne out by the fact that with the second film the maximum pressure during the evaporation was  $5 \times 10^{-8}$  millimeters, yet essentially the same results were obtained.

Since silver was the first metal studied, the results were carefully examined for instrumental effects. It was found that the thermal time constant of the system limited the time in which a cycle could be traversed. When the heater input was disconnected, the cylinder cooled uniformly because cooling was primarily by radiation. Since the sides of the cylinder were nearer the heater coil than the end, when the film was heated rapidly, the sides of the cylinder became temporarily much hotter than the ends. The thermocouple readings were thus in considerable error until equilibrium was established by conduction. Since the equilibrium values of the contact potential agreed with the equilibrium thermocouple readings, the transient discrepancy was not due to contamination. Temperature differences at equilibrium were small, since tests on a similar system showed a maximum variation of 35 degrees over the whole cylinder when the cylinder was at a mean temperature of  $900^{\circ}\text{C}$ .

A small change in contact potential was measured when the vibrator was excited at different amplitudes. This was probably due to pick-up of second harmonic from the exciting system. Usually the vibrator was excited until it stopped just short of the fixed plate, and was maintained at this amplitude throughout the evaporation and subsequent readings. Readings could be obtained, however, with less sensitivity at much smaller

amplitudes. Tests at large and small amplitudes on a stable film one week old resulted in a measured variation of 23 millivolts in contact potential, but no significant difference in the measured value of the temperature coefficient. The values of  $\frac{dV_{21}}{dT}$  were 118 and 113 microvolts per degree Kelvin for large and small amplitudes respectively. It is interesting to note that the temperature coefficient of this week-old film was still very close to the values obtained from freshly-prepared films.

Measurements on copper were similar to those on silver. Evaporation of the copper had to be performed at a higher temperature, however, than was needed in the case of silver. Out-gassing was therefore a greater problem and pressures during the evaporation were higher. When the first bead (Bead I) was used, the maximum pressure during the evaporation was  $1.5 \times 10^{-7}$  millimeters of mercury. When the evaporation was stopped, the pressure dropped a factor of 10 in approximately 10 seconds. Measurements could therefore be taken almost immediately at pressures near  $10^{-9}$  millimeters of mercury. The maximum pressures during the evaporation of the other two films were  $10^{-7}$  and  $6 \times 10^{-8}$  millimeters of mercury. These films were prepared successively from a second bead (Bead II). Measurements on one of these films were extended over a period of six hours without any measured drift in contact potential.

Further readings could not be obtained from Bead I because the bead was overheated in attempting the next evaporation. Strain relief occurred in the bead supports and moved the bead under the cylinder where no coverage of the end was possible. The results shown in Figure 7 for Bead I were transposed -0.200 volts to allow the results to appear on the same graph. The position of the bead in this case was probably the cause of the large difference in contact potential. In the other cases the bead

was placed where, with the vibrator operating, the bead evaporated on both sides of the vibrator as well as the end of the cylinder. Since the vibrating plate was smaller than the fixed plate, appreciable capacitive coupling to the far side of the vibrating plate must have occurred. This was verified by measurements made on a resistive network analogue computer. Thus the measurement in which this side did not have an evaporated coating yielded a different value of contact potential, but the same temperature coefficient.

The results of measurements made on gold films were not as satisfactory as those made on silver or copper films. Due to the fact that appreciable evaporation of gold only took place at higher temperatures than were needed for evaporating silver or copper, more difficulty was encountered in out-gassing the bead. Table V lists the results obtained from the gold films. A value of  $-\frac{dV_{21}}{dT}$  of approximately 100 microvolts/°K was measured for the average temperature coefficient of the fifth, sixth and seventh films evaporated. A smaller temperature coefficient was observed when the film produced from the last of the bead was examined, but this portion of the bead probably contained a higher concentration of impurities. During the last evaporation the tungsten basket was kept at a high temperature for two or three minutes after the bead had evaporated. The temperature coefficient observed agreed with the experimental values for tungsten observed by Potter<sup>9</sup>. The results listed in Table VI were obtained by drawing a line by inspection through a plot of the experimental results.

The least square method was used to analyse the observations made on silver and copper films. This was done to obtain an objective measurement of the temperature coefficient and an estimate of the probable error introduced by the scatter of the experimental results.

TABLE V

Values of  $-\frac{dV_{21}}{dT}$  Measured from Successively Deposited Gold Films

Film	$-\frac{dV_{21}}{dT}$ (Microvolts/°K)	Pressure During Evaporation (mm Hg)	Remarks
1	157	$4 \times 10^{-8}$	
2	310	$1.8 \times 10^{-7}$	Considerable drift.
3	260 217	$2 \times 10^{-8}$	One week after preparation.
4	215 160	$1.2 \times 10^{-7}$	One week later.
5	130 90	$5 \times 10^{-8}$ )	Considerable drift. Mean of 110.
6	110 70	$1 \times 10^{-7}$ )	Considerable drift. Mean of 90.
7	100 103 107	$1 \times 10^{-8}$	Amplitude of vibration reset. Two weeks after preparation.
8	70	$1 \times 10^{-7}$	Bead nearly evaporated.
9	63	$\sim 10^{-6}$	Results agree with value for tungsten.

TABLE VI  
Results of Least Square Calculations

	$-\frac{dV_{21}}{dT}$	$-V_{21}$	Probable Error in Individual Readings
	$10^{-6} \text{ V}/^\circ\text{K}$	Volts	Volts
<u>Silver</u>	$-131 \pm 3$	0.113 at 300°C	0.004
	$-123 \pm 4$	0.095 at 250°C	0.002
Mean	$-127 \pm 4$		
<u>Copper</u>			
Bead I	$-48 \pm 1$	0.216 at 250°C	0.002
Bead II	$-51 \pm 2$	0.040 at 300°C	0.002
	$-51 \pm 2$	0.022 at 300°C	0.002
Mean	$-50 \pm 2$		

TABLE VII

Comparison of Theory and Experiment

	$(d\phi/dT)_{Z'=0}$	$(d\phi/dT)_{Z'=1}$	$(d\phi/dT)_{\text{expt.}}$	$Z'$
	$10^{-5} \text{ eV}/^\circ\text{K}$			
Cu	-0.5	-17	-5.7	0.32
Ag	-0.4	-15	-13.4	0.88
(Au)	0.4	-13	$\sim 9$	....

The mathematical treatment of these measurements is discussed in Appendix III. Table VI lists the results of the least square calculations. These results still require correction for the absolute thermoelectric power of the circuit connecting the two condenser plates. Since the electrical connection to the heated plate was made at the cold junction of the platinum thermocouple wire, the experimental results should be corrected for the absolute thermoelectric power of platinum. This correction is  $-7.3$  microvolts per degree (Reference 37).

Table VII lists the temperature coefficients expected, assuming first that all the valence electron charge density vibrates rigidly with the ion cores ( $Z' = 0$ ), and secondly that the valence electrons are completely independent of the ion core vibrations ( $Z' = 1$ ). The experimental temperature coefficients for copper and silver lie between the two as might be expected. The last column shows the effective value of the vibrating charge.

The results from the gold films cannot be explained by the theory since only negative temperature coefficients can be interpreted as determining a value of  $Z'$ .

The chief criterion to be used in judging the merits of the results is the reproducibility of the temperature coefficient of successively prepared films and the absence of drift in the contact potential measurements. The results obtained using copper and silver films are thus acceptable, but the above criterion rejects the results taken from films prepared previous to seal-off and the results from gold films. The films prepared previous to seal-off yielded dubious results because of their instability at high temperatures, and the results from gold films were unreliable because of both drift and lack of reproducibility.

Two possible reasons can be offered to explain why the results

from gold films were not as reproducible as those from copper and silver films. The gold sample may not have been sufficiently pure. Evaporation would then have deposited films of changing composition. A second possible explanation is that the expansion and contraction of the nickel substrate may have set up strains in the gold films which did not exist in the copper and silver films, since the expansion coefficients of these metals match that of nickel more closely than does the expansion coefficient of gold. A much thicker layer of gold would then have been necessary to eliminate the effect of the substrate. The latter explanation of the results from gold films suggests that future experiments be done using substrates of the metal being evaporated.

## CONCLUSIONS

Theoretical expressions applicable to the monovalent metals have been derived for the effect of thermal expansion and for the effect of thermal vibration at constant volume on the chemical potential. It was found that the theoretical values of these two effects virtually cancel at all temperatures. Since the effect of the electronic specific heat is negligible for monovalent metals, the only important net contribution to the temperature dependence of the work function was found to be the electrostatic effect of ion core vibrations.

Experimental measurements of the temperature dependence of the work functions of the monovalent noble metals have been made using a capacitive contact potential method. These measurements were taken in sealed-off systems under conditions where the contaminating effects of residual gas could be detected if present. Measurements on evaporated silver and copper films were free from contamination effects and reproducible, while measurements on gold films were not satisfactory in either respect.

The experimental results from copper and silver films can be explained by the theory which was developed, but the less reliable results from gold films are not consistent with the theory. Possible explanations for these results are impurities in the gold or a lack of a thick enough film to eliminate the effect of strains due to differential expansion of the nickel substrate and the gold film.

The theory can be subjected to several additional experimental checks. Measurements should be made of the temperature dependence of the work functions of the alkali metals. The low temperature variation of the work function should also be investigated since the form of this

variation is predicted by the Debye theory for the ion core vibrations. The temperature coefficients of different crystal faces of a metal are also of interest because of the data which can be obtained about the properties of surface dipole layers. Smoluchowski's theory predicts a relatively small difference in the temperature coefficients of different crystal faces, but this theory still needs experimental verification.

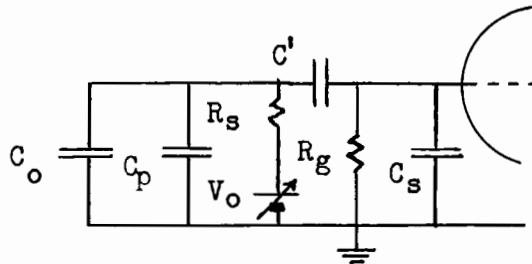
## APPENDIX I

## Sensitivity of the Dynamic Capacitive Method

The dynamic capacitive method or Zisman<sup>38</sup> method is capable of great sensitivity. With suitable geometry and associated circuits, contact potential changes of the order of  $10^{-5}$  volts have been measured<sup>39</sup>.

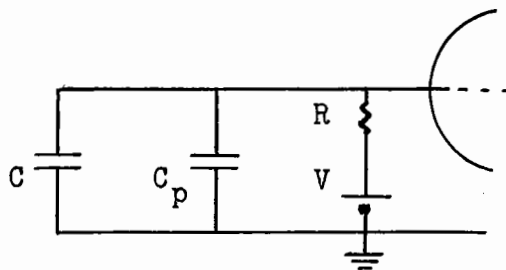
The dynamic capacitive method is a modification of the Kelvin method of measuring contact potential. In the Kelvin method a transient change in capacitance between two metal surfaces produces in the circuit connecting them, a flow of charge proportional to the contact potential. In the Zisman method the capacitance change is periodic and an alternating current flows in the circuit connecting the surfaces. If an opposing direct e.m.f. is inserted in the circuit, the charging currents are reduced to zero when the opposing voltage is the same size as the contact potential. The contact potential can thus be measured by a null method. This method is capable of greater sensitivity than the Kelvin method because selective amplifiers can be used to decrease the noise in the null detecting system.

The circuit used in the Zisman method is shown below.



$C_o$  is the static capacitance between the vibrating plate and the fixed plate,  $C_p$  the periodic portion of the capacitance,  $C_s$  the input stray capacitance of the null detector, and  $V_o$  the voltage opposing the

contact potential difference. The equivalent circuit for generating an alternating voltage at the input of the detector is shown below.



Since the impedance of  $C'$  should be negligible,

$$C = C_0 + C_s \quad \text{and} \quad R = R_s R_g / (R_s + R_g) \quad (58)$$

$V$  is the difference between the contact potential and  $V_0$ . Now

$$V = q / (C + C_p) + R dq/dT \quad (59)$$

$q$  is the charge on the condenser. If the period of the capacitance change is  $2\pi/\omega$ ,  $C_p$  can be expressed as

$$C_p = \sum_{n=1}^{\infty} C_n \exp j(n\omega t + \alpha_n) \quad (60)$$

and  $q$  by the series,

$$q = \sum_{n=0}^{\infty} q_n \exp j(n\omega t + \beta_n) \quad (61)$$

The largest harmonic of  $q$  is the only term of interest when a selective null detector is used. When  $C_1$  is the largest component of  $C_p$ , and

$C \gg C_p$ , then the alternating voltage across  $R$  has an amplitude

$$e_R = \frac{V \omega C_1 R}{[1 + (\omega CR)^2]^{1/2}} \quad (62)$$

and a phase relative to that of  $C_1$  of  $-\tan^{-1} \omega CR$ . For a given unbalance  $V$ , the maximum value of  $e_R$  is

$$e_R = VC_1/C \quad (63)$$

when  $\omega CR \gg 1$ . Since the stray capacitance across  $C_0$  is a part of  $C$ , for good sensitivity, stray capacitances should be kept at a minimum. The signal-to-noise ratio, however, is not a function of  $C$ . If the detector has an effective noise bandwidth  $B$  and a noise figure  $N$ , the amplitude of the r.m.s. noise voltage across the input is

$$e_N = \left[ \frac{4kTBEN}{1 + (\omega CR)^2} \right]^{1/2} \quad (64)$$

and the signal-to-noise ratio is

$$e_R/e_N = V \omega C_1 (R/4kTEN)^{1/2} \quad (65)$$

When  $R = 2 \times 10^7$  ohms,  $\omega = 240$  radians per second,  $C_1 = 10^{-13}$  farads,  $B = 1$  cycle,  $N = 1$  and  $T = 300^\circ\text{K}$ , the voltage unbalance is 1 millivolt when the signal-to-noise ratio is unity. These were the approximate operating conditions for the final experimental arrangement.

## APPENDIX II

## The Time for Contamination of Clean Surfaces

An idea of the time required to contaminate a clean surface can be obtained from the following simple model of the process of contamination.

If a fraction  $f$  of a surface under consideration is covered by a monolayer of contamination, and if the average work function is determined by the percentage of clean and contaminated areas, the arithmetic mean of the work function is

$$\phi = f\phi_c + (1 - f)\phi_o \quad (66)$$

where  $\phi_o$  is the work function of the clean surface and  $\phi_c$  that of the contaminated surface. Assuming the rate of contamination is proportional to the area of clean surface exposed,

$$df/dt = (1 - f)/\tau \quad (67)$$

and

$$f = 1 - \exp -t/\tau \quad (68)$$

$\tau$  is the time constant of the contamination process. Thus

$$d\phi/dt = \exp(-t/\tau)(\phi_c - \phi_o)/\tau \quad (69)$$

If the molecules of the contaminating gas have a Maxwellian distribution of velocities, the number of molecules incident on unit

surface per unit time at a pressure  $P$  is

$$n = P/(2\pi MkT)^{1/2} \quad (70)$$

$M$  is the mass per molecule of the incident gas. If a fraction  $\bar{r}$  of these molecules is reflected, and the molecules adhering to the surface each occupy an area  $d^2$ ,

$$\tau = \frac{1}{(1 - \bar{r})d^2 n} = \frac{\sqrt{2\pi MkT}}{(1 - \bar{r})Pd^2} \quad (71)$$

If  $M$  is measured in atomic units,  $T$  in degrees Kelvin,  $P$  in millimeters of mercury,  $d$  in angstroms and  $\tau$  in minutes,

$$\tau = \frac{4.75 \times 10^{-8} (MT)^{1/2}}{(1 - \bar{r})Pd^2} \quad (72)$$

If  $M = 32$ ,  $T = 300^\circ\text{K}$ ,  $\bar{r} = 0$ ,  $P = 10^{-8}$  millimeters of mercury, and  $d = 2$  angstroms;  $\tau = 12$  minutes. Thus if  $\phi_c - \phi_o = 1$  eV, the initial drift in the mean work function of a freshly prepared clean surface is  $89 \times 10^{-3}$  eV per minute. Figure 8 shows the initial drift as a function of pressure for various values of  $\phi_c - \phi_o$  assuming the other parameters in Equation (72) are as listed above.

When making measurements of the temperature coefficient of the work function of a metal, contact potential changes of the order of a few millivolts must be measured, hence the importance of maintaining a

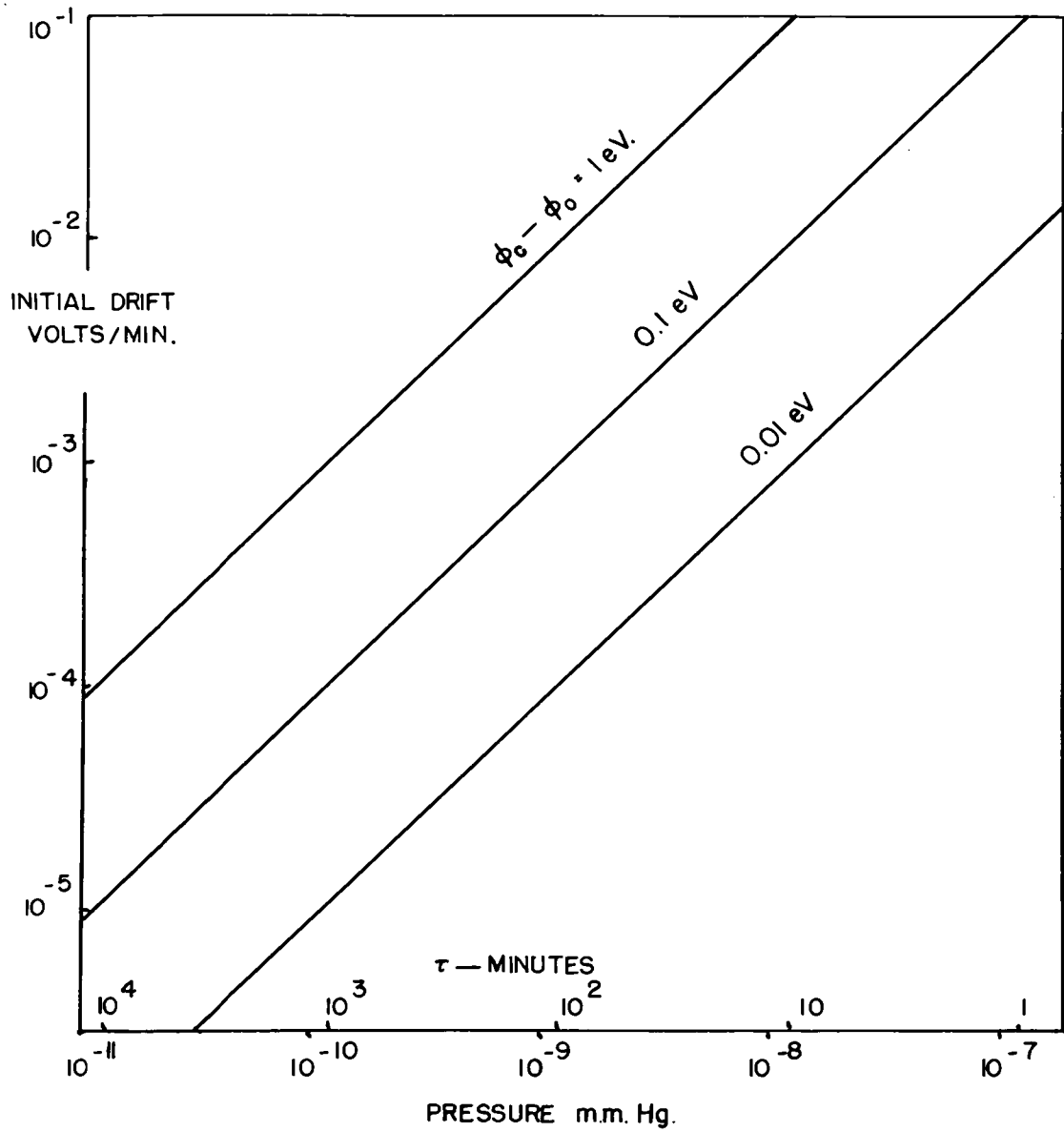


Figure 8 - Contamination Effects of Residual Gases

low partial pressure of contaminants cannot be overemphasized. At the same time, however, it should be noted that the reflection coefficient of molecules of inert gases is essentially unity (i.e., they have little or no contaminating effect), and in well-gettered sealed-off systems the active contaminants are removed preferentially. Since molecules of the inert gases contribute to the pressure indication of an ionization gauge, the readings of ion gauges under these conditions can only be accepted as an indication of the maximum possible partial pressure of contaminating gases. Thus when the minimum possible contamination time is of the order of the time during which a drift in work function can be observed, the best criterion of freedom from continuing contamination is freedom from drift in the measurements themselves. The ionization gauge reading is definitely of value, however, for measurements at high pressures may be reproducible and free from drift simply because the surfaces examined have reached a stable state of contamination before measurements have started.

## APPENDIX III

## Analysis of Results

The least square method was used to analyse the observations obtained from copper and silver films. When using this method it is assumed that the line of best fit through an assembly of points is the one which minimizes the sum of the squares of the deviations of the points. Thus if  $y = a + bx$  is the line of best fit and the  $i$ th measured point is  $x, y_i$

$$\sum_{i=1}^n [y_i - (a + bx)]^2 = 0 \quad (73)$$

Then

$$\frac{\partial}{\partial a} \sum_{i=1}^n (y_i - y)^2 = 0 \quad (74)$$

and

$$\frac{\partial}{\partial b} \sum_{i=1}^n (y_i - y)^2 = 0 \quad (75)$$

These equations reduce to

$$a = \frac{\sum x \sum xy_1 - \sum x^2 \sum y_1}{(\sum x)^2 - n \sum x^2} \quad (76)$$

and

$$b = \frac{\sum x \sum y_1 - n \sum xy_1}{(\sum x)^2 - n \sum x^2} \quad (77)$$

The probable error in a single reading is

$$P_i = 0.675 \left[ \frac{\sum (y_i - y)^2}{n - 2} \right]^{1/2} \quad (78)$$

and the probable errors in a and b are

$$\begin{aligned}
 P_a &= P_1 \left[ \frac{\sum (x \sum x - \sum x^2)^2}{(\sum x^2 - n \sum x^2)^2} \right]^{1/2} \\
 &= \frac{P_1}{\left[ n - (\sum x)^2 / \sum x^2 \right]^{1/2}} \quad (79)
 \end{aligned}$$

and

$$\begin{aligned}
 P_b &= P_1 \left[ \frac{\sum (nx - \sum x)^2}{((\sum x)^2 - n \sum x^2)^2} \right]^{1/2} \\
 &= \frac{P_1}{\left[ \sum x^2 - \frac{(\sum x)^2}{n} \right]^{1/2}} \quad (80)
 \end{aligned}$$

A total of approximately three hundred observations were recorded in obtaining the results for silver and copper. The labour of direct least square calculations was therefore prohibitive. A close approximation was used which made the calculations relatively simple. The temperature range investigated was divided into identical intervals. The results were then plotted and the slope determined by inspection. This slope was used to alter each reading to its value had it been taken at the centre of the interval in which it fell. The average reading in each group was then determined. These averages are the points plotted in Figure 7, and listed in Table VIII. In calculating a and b, the group average was given a weight corresponding to the number of readings

TABLE VIII

Data for Least Square Determination of  $-dV_{21}/dT$ 

<u>Silver</u>						
Temperature ( $^{\circ}\text{C}$ )	100	200	300	400	500	
$-V_{21}$ (Volts)	0.138	0.127	0.113	0.094	0.087	
Number of Readings	21	17	10	11	31	
<u>Copper</u>						
Bead I						
(Transposed $-0.200$ Volts on graph)						
Temperature ( $^{\circ}\text{C}$ )	50	150	250	350	450	550
$-V_{21}$ (Volts)	0.225	0.221	0.217	0.211	0.206	0.203
Number of Readings	6	11	6	10	11	11
Bead II						
Temperature ( $^{\circ}\text{C}$ )	100	200	300	400	500	
$-V_{21}$ (Volts)	0.050	0.045	0.038	0.034	0.030	
Number of Readings	10	7	5	8	8	
Temperature ( $^{\circ}\text{C}$ )	0	100	200	300	400	500
$-V_{21}$ (Volts)	0.038	0.032	0.028	0.022	0.018	0.011
Number of Readings	7	17	9	9	12	34

in the group. The individual modified readings were used to calculate  $P_i$  once  $a$  and  $b$  were known.

The above procedure is exact if the slope determined by inspection is the same as that obtained from the least square calculation. When  $b$  is large the possibility of error is greater than when  $b$  is small, but even in the case of the readings from silver films, a ten percent error in the temperature coefficient over a fifty degree temperature range would only cause an error of 0.7 millivolt in a modified contact potential reading. This error would also only apply to a small minority of points and would cancel if the original assembly of points were symmetrically scattered over both halves of the temperature interval.

An illustration of this treatment is shown in Table IX using the original observations and modified readings obtained from the first copper bead. These are listed in the order in which they were taken. The original observations are plotted in Figure 9.

The least square analysis cannot eliminate a systematic error introduced by heating of the reference surface. This error was presumed to be small because with the tube envelope at  $450^{\circ}\text{C}$  and the heated condenser plate at  $875^{\circ}\text{C}$ , the reference plate was not even faintly red, which meant that its temperature was near that of the tube envelope and not more than  $500^{\circ}\text{C}$ . Heating of the reference electrode would decrease the effective temperature difference and yield small experimental temperature coefficients. In the cases of silver and copper, experimental temperature coefficients corrected for this error would thus be closer to the theoretical values for  $Z' = 1$ .

TABLE IX

## Original and Modified Observations on Copper (Bead I)

Original (Millivolts)	Temperature (°C)	Modified (Millivolts)	Temperature (°C)
202	557	202	550
200	551	200	550
204	551	204	550
207	546	207	550
204	546	204	550
208	457	208	450
208	428	207	450
210	417	209	450
211	417	210	450
214	347	214	350
214	335	213	350
214	318	212	350
217	306	215	350
219	243	219	250
220	212	218	250
222	206	220	250
222	206	220	250
220	173	221	150
220	159	220	150
220	159	220	150
223	124	222	150
224	110	222	150
223	102	221	150
224	87	226	50
224	79	225	50
224	79	225	50
224	71	225	50
225	63	226	50
224	71	225	50
223	124	222	150
224	139	223	150
222	152	222	150
216	166	217	150
219	173	220	150
214	243	214	250
213	263	214	250
214	287	216	250
210	306	208	350
210	324	209	350
210	335	209	350
210	347	210	350
210	347	210	350
205	382	207	350

(continued on page 68)

Table IX, continued

Original (Millivolts)	Temperature (°C)	Modified (Millivolts)	Temperature (°C)
202	411	200	450
203	445	203	450
204	451	204	450
202	462	203	450
205	462	206	450
204	462	205	450
208	486	210	450
202	546	202	550
200	551	200	550
207	551	207	550
204	551	204	550
205	551	205	550
202	551	202	550

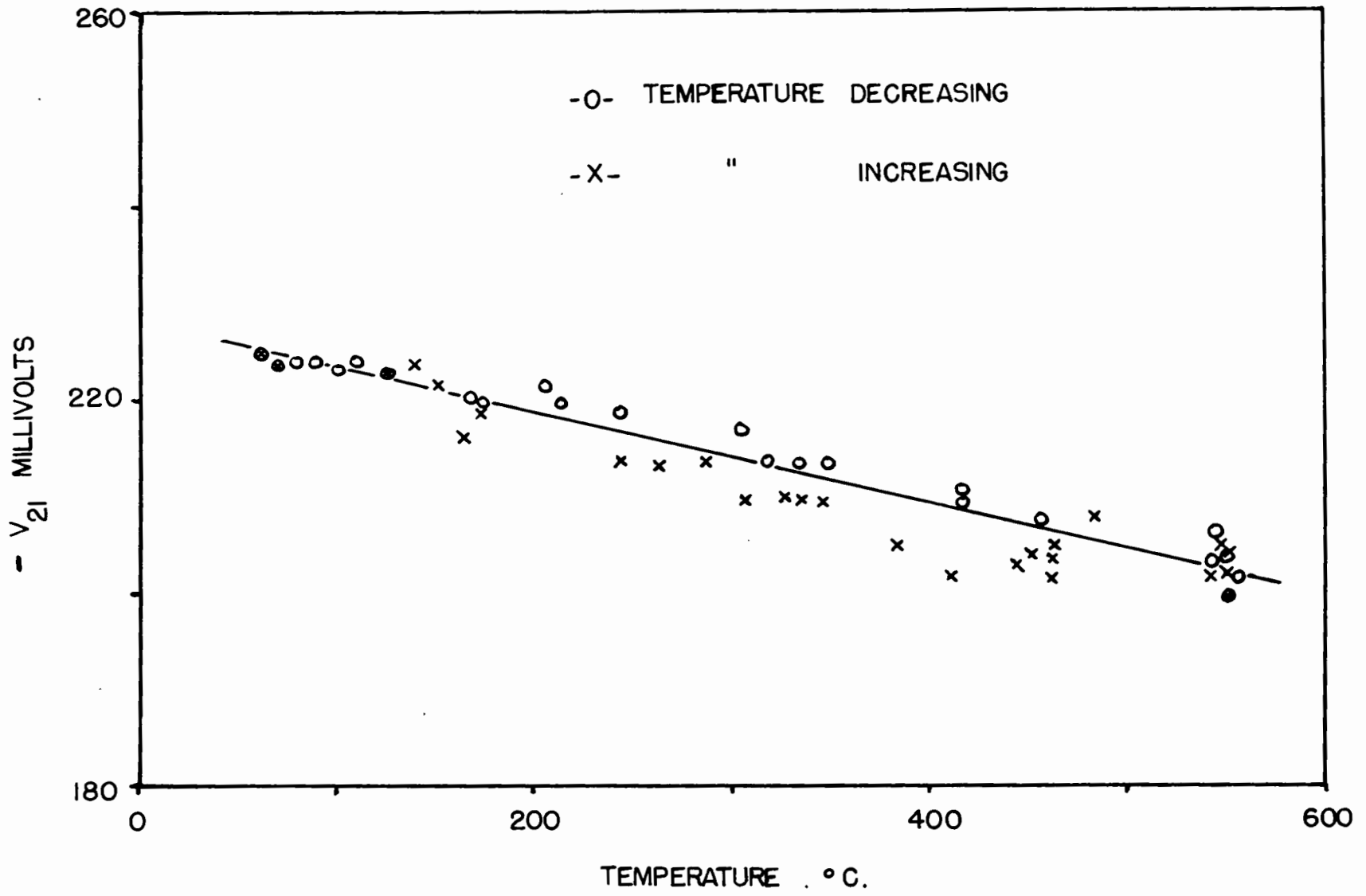


Figure 9 - Experimental Observations on Copper (Bead I)

## REFERENCES

1. Herring, C. and Nichols, M.H., Rev. Mod. Phys., 21, 185, (1949).
2. Smoluchowski, R., Phys. Rev., 60, 661, (1941).
3. Wigner, E.P. and Bardeen, J., Phys. Rev., 48, 84, (1935).
4. Bardeen, J., Phys. Rev., 49, 653, (1936).
5. Blochinzev, D. and Drabkina, S., Physik Z. Sowj., 7, 484, (1935).
6. Underwood, N., Phys. Rev., 47, 502, (1935).
7. Farnsworth, H.E., and Winch, R.P., Phys. Rev. 58, 812, (1940).
8. Mendenhall, C.E. and deVoe, C.F., Phys. Rev., 51, 346, (1937).
9. Potter, J.G., Phys. Rev., 58, 623, (1940).
10. Richardson, O.W., Phil. Mag., 23, 594, (1912).
11. Herzfeld, K.F., Phys. Rev., 35, 248, (1930).
12. Riemann, A.L., Nature, 133, 833, (1934).
13. Wigner, E.P., Phys. Rev., 49, 696, (1936).
14. Seely, S., Phys. Rev., 59, 75, (1941).
15. Wigner, E.P., Phys. Rev. 46, 1002, (1934).
16. Seitz, F., Modern Theory of Solids, (McGraw-Hill, New York, 1940).
17. Seitz, F., Phys. Rev., 47, 400, (1935).
18. Wigner, E.P. and Seitz, F., Phys. Rev., 46, 509, (1934).
19. Gorin, E., Physik Z. Sowj., 9, 328, (1936).
20. Fuchs, K., Proc. Roy. Soc., 151, 585, (1935).
21. Jones, H. and Mott, N.F., Proc. Roy. Soc., 162, 491, (1937).
22. Mott, N.F., Proc. Phys. Soc., 152, 42, (1935).
23. Stoner, E.C., Phil. Mag., 21, 145, (1936).
24. Sun, N.T., and Band, W., Proc. Camb. Phil. Soc., 42, 72, (1946).

25. Wohlfarth, E.P., Proc. Phys. Soc., 60, 360, (1948).
26. McDougal, J. and Stoner, E.C., Phil. Trans., A257, 67, (1939).
27. Slater, J.C., Introduction to Chemical Physics, (McGraw-Hill, New York, 1939).
28. Recueil de Constantes Physique-Societe Francaise de Physiques, Paris, (1912).
29. Wyckoff, R., Crystal Structure, Vol. I, (Interscience Publishers, Inc., New York, 1948).
30. Hermann, I.G. and Wagener, P.S., The Oxide-Coated Cathode, Vol. II, (Chapman and Hall, Ltd., London, 1951).
31. Jain, S.C. and Krishnan, K.S., Proc. Roy. Soc., A217, 451, (1954).
32. Kruger, F. and Stabenow, G., Ann. d. Physik, 22, 713, (1935).
33. Langmuir, D. B., Phys. Rev., 49, 428, (1936).
34. Cardwell, A.B., Phys. Rev., 47, 628, (1935).
35. DuBridge, L.A. and Roehr, W.W., Phys. Rev., 42, 52 (1932).
36. Herring, C., Phys. Rev., 59, 889, (1941).
37. Mott, N.F., Proc. Roy. Soc., A156, 368, (1936).
38. Zisman, W.A., Rev. Sci. Instrum., 3, 367, (1932).
39. Philips, G., J. Sci. Instrum., 28, 342, (1951).

## ACKNOWLEDGMENTS

The author wishes to acknowledge the aid and encouragement given him by his research director, Professor G. A. Woonton, and also by Dr. R. Sharp, who made several valuable suggestions which clarified the presentation of the theory. The author is also indebted to Mr. R. Lorimer who did the glass-blowing for this project, and to his colleagues at the Eaton Electronics Research Laboratory with whom he had many valuable discussions.

This research was made possible through the use of equipment purchased by a Defence Research Board grant which also covered the author's salary as a research assistant during a term of summer employment.